Aqueous Systems at Elevated Temperatures and Pressures:
Physical Chemistry in Water, Steam and Hydrothermal Solutions
D.A. Palmer, R. Fernández-Prini and A.H. Harvey (editors)

Chapter 10

Transport properties in high temperature and pressure ionic solutions

Horacio R. Corti,[a,*] Liliana N. Trevani[b] and Andrzej Anderko[c]

[a] *CNEA, Buenos Aires, Argentina*
[b] *University of Guelph, Guelph, Ont., Canada*
[c] *OLI Systems, Morris Plains, NJ, USA*

10.1. Introduction

This chapter is devoted to the study of transport properties in aqueous ionic solutions at elevated temperatures and pressures. The electrical conductivity and the diffusion of salts and their ionic components will be analyzed as a function of temperature and density (pressure) over the entire concentration range, from infinite dilution to very concentrated solutions.

The viscosity and thermal conductivity of ionic solutions will also be analyzed in relation to the salt effect as a function of the state variables. Special attention is paid to predictive models to estimate the values of the transport coefficients over a wide range of temperature, pressure and electrolyte concentration.

10.2. Basic Definitions and Phenomenological Equations

The transport coefficients that we will deal in this chapter have been defined in connection with the phenomenological laws that describe the transport of charge, mass or momentum in electrolyte solutions. These laws and the main characteristics of the transport parameters will be summarized briefly.

We assume that the aqueous system contains an electrolyte $A_{\nu_-}C_{\nu_+}$ of molar concentration c, which dissociates according to

$$A_{\nu_-}C_{\nu_+}(\mathrm{aq}) \rightleftharpoons \nu_- A^{z-}(\mathrm{aq}) + \nu_+ C^{z+}(\mathrm{aq}) \tag{10.1}$$

yielding ionic concentration $c_i = \alpha \nu_i c$, where α is the degree of dissociation of the electrolyte and ν_i the stoichiometric number. The charges of the anion and cation

* Corresponding author. E-mail: hrcorti@cnea.gov.ar

are z_- and z_+, respectively. It is also assumed that the electric neutrality condition holds, that is,

$$z_+c_+ + z_-c_- = z_+\nu_+ + z_-\nu_- = 0. \tag{10.2}$$

The ions may also associate in solution to form an ion pair, according to the equilibrium

$$A^{z-}(\text{aq}) + C^{z+}(\text{aq}) \rightleftharpoons AC^{(z_+ + z_-)}(\text{aq}), \tag{10.3}$$

with K_A being the thermodynamic constant associated with the ion-pair formation reaction. In symmetric electrolytes ($\nu_+ = \nu_-$), such as NaCl or $MgSO_4$, the ion pairs are neutral species, while in unsymmetrical electrolytes, such as $MgCl_2$, they bear a net charge.

Some of the transport phenomena, such as diffusion and electrical conductivity, involve fluxes of solute species (ionic and non-ionic) in the solvent. Therefore, it is possible to give a general expression for these molecular fluxes in terms of the concentration and velocity, independent of the driving force that causes the molecular mobility in the solution.

In a system formed by solute particles (concentration c_i) moving with velocity v_i in a solvent which moves with a convective velocity v_C, the molar flux $\mathbf{J}_i$ (the number of moles transported per unit area per time relative to fixed coordinates) is given by

$$\mathbf{J}_i = c_i(v_i - v_C). \tag{10.4}$$

The convective flow is not necessarily due to external forces on the whole system; it could originate in the local flow of solvent associated with the solute molecules flowing in solution (Fig. 10.1).

If the solute species are ions bearing charge z_i, the total flow of charge is

$$\mathbf{J}_q = \sum_{i=1} z_i F \mathbf{J}_i \tag{10.5}$$

where F is the Faraday constant, 96,485 Coulombs/mol and the summation is over all ionic species. This charge flow is called the current density, i, defined as the electric charge transported per unit of time and area.

The macroscopic equations which relate the flow of mass (diffusion) and current density (conductivity) to the driving forces in the system are Fick's equation and Ohm's equation, respectively, shown in Table 10.1. Other transport properties, such as the flow of momentum (viscosity) and heat (thermal

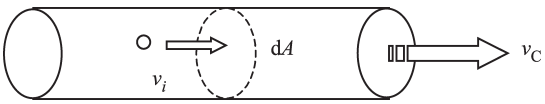

Fig. 10.1. Molecular flux across an arbitrary plane in a fluid system moving with velocity v_C.

Table 10.1
Macroscopic equations for the main transport properties

Property	Driving force	Transport coefficient	Relationship
Mass transport	Concentration gradient	Diffusion coefficient (D)	Fick $J = -\mathrm{D}\ \mathrm{grad}\ c$
Charge transport	Potential gradient or electric field ($E = \mathrm{grad}\ \phi$)	Specific conductivity (κ)	Ohm $J_q = i = \kappa\ \mathrm{grad}\ \phi$
Momentum transport	Shear stress	Viscosity (η)	Poiseuille $p_{xy} = -\eta\ \mathrm{grad}\ v_x$
Heat transport	Temperature gradient	Thermal conductivity (λ)	Fourier $J_Q = -\lambda\ \mathrm{grad}\ T$

conductivity) involve both the solvent and the solute molecules, so that transport occurs even in the absence of solute. The relationship between flows and driving forces for these transport properties is also summarized in Table 10.1.

A general formalism of irreversible transport processes was developed by Onsager (1931a–c) in terms of fluxes, $\mathbf{J}_i$, which are linearly related to generalized driving forces, $\mathbf{X}_j$, by

$$\mathbf{J}_i = \sum_{j=1}^{n} a_{ij}\mathbf{X}_j \ (i = 1, 2, \ldots, n) \tag{10.6}$$

where a_{ij} are phenomenological coefficients, dependent on the thermodynamic state variables, which approach zero as $c_i \rightarrow 0$. Onsager showed by using the Principle of Microscopic Reversibility that

$$a_{ij} = a_{ji} \ (i, j = 1, 2, \ldots, n). \tag{10.7}$$

These are the Onsager Reciprocity Relations (ORR), which allow us to reduce the number of independent phenomenological coefficients required to describe the irreversible processes taking place in a system subjected to several driving forces.

10.2.1. Electrical Conductivity

In electrolyte solutions, the charge is transported by ions moving under the influence of an electric field, E, equal to the gradient of the electrical potential gradient. The specific conductivity, κ, is defined by Ohm's law (Table 10.1), and it could be expressed in terms of the resistance R of a parallelepiped of solution of area A and length l as $\kappa = l/AR$. That is, κ is the conductance (inverse of resistance) per unit of area and length and its unit is S cm^{-1}.

While in solid conductors κ is a constant, under constant pressure and temperature, in electrolyte solutions κ becomes a parameter depending on the ionic

concentration and also on the electric mobility, u_i, of these ions in the solution. The ionic electric mobility is defined as $u_i = (v_i - v_R)/E$, and it depends on the reference system adopted to measure the ionic velocities. For instance, the reference velocity could be the average velocity of the solvent molecules, called Hittorf's reference system (for a discussion of different reference systems see Haase, 1990).

For a binary electrolyte solution, the specific conductivity is given by (Haase, 1990)

$$\kappa = F(c_+|z_+|u_+ + c_-|z_-|u_-) = (\nu_+|z_+|\lambda_+ + \nu_-|z_-|\lambda_-)\alpha c \tag{10.8}$$

where $\lambda_i = Fu_i$ is the ionic conductivity of the i ion.

In order to eliminate the explicit concentration dependence, the equivalent conductivity, Λ, is defined in terms of the equivalent concentration, $c^* = \nu_+|z_+|c = \nu_-|z_-|c$,

$$\Lambda = \frac{\kappa}{c^*} = \alpha(\lambda_+ + \lambda_-). \tag{10.9}$$

In the modern literature, following the recommendations of IUPAC, the equivalent conductivity has been replaced by the molar conductivity (κ/c) of the $(1/\nu_+z_+)A_{\nu_-}C_{\nu_+}$ substance (Fernández-Prini and Justice, 1984) which, taking into account the relationship between c^* and c, has the same numerical value as the old-fashioned equivalent conductivity.

At the infinite dilution limit ($c \to 0$), the ion mobility only depends on the ion–solvent interactions and the ionic and the molar conductivities reach their infinite dilution values λ_i^0 and Λ^0, respectively. Because the dissociation is complete as the concentration goes to zero, the molar conductivity at infinite dilution can be written as

$$\Lambda^0 = \lambda_+^0 + \lambda_-^0 \tag{10.10}$$

known as Kohlrausch's law of independent ion migration. It simply indicates that at infinite dilution the ionic mobility of a given ion is independent of the type of salt, that is, of the nature of the counterion.

The generalization of these quantities to a multicomponent system with n electrolytes is straightforward, but we must be careful with notation because some electrolytes could have common ions. Thus, a system with n electrolyte components will have N ionic components, with $N \leq 2n$, and the following expression is valid

$$\Lambda = \frac{\sum_{k=1}^{n} \kappa_k}{\sum_{k=1}^{n} c_k} = \frac{\sum_{i=1}^{N} c_i|z_i|\lambda_i}{\sum_{i=1}^{N} c_i} \tag{10.11}$$

where c_k are the concentrations of the constituent electrolytes and c_i are the ionic concentrations. It is important to note that, due to the electroneutrality condition, the total current density and therefore κ and Λ are independent of the reference system.

In the Onsager formalism, the driving force for the electrical conductivity is the electric potential gradient, $\mathbf{X} = -\text{grad}\ \phi$, and the phenomenological equation for specific conductivity is

$$\kappa = F^2 \sum_i \sum_k z_i z_k a_{ik} \tag{10.12}$$

where the sum is over all the ions in solution. The expression for the ionic conductivity is

$$\lambda_i = \frac{F^2}{c_i} \left| \sum_k a_{ik} z_k \right| \tag{10.13}$$

which makes clear the effect of other ions on the mobility of the ion i, indicated by the cross coefficients a_{ik} $(i \neq k)$.

10.2.2. Transport Numbers

It is clear from Eq. 10.8 that each ion makes its own contribution to the total current density. The transport or transference number measures the fraction of the total current transported by a given ion in the solution, and it is defined as

$$t_i = \frac{i_i}{i} = \frac{|z_i| c_i u_i}{\sum_i |z_i| c_i u_i} = \frac{|z_i| \nu_i \lambda_i}{\Lambda}. \tag{10.14}$$

An obvious consequence of the definition is that $\sum t_i = 1$. While the total current is independent of the reference system, the partial or ionic current is not. The Hittorf reference system is commonly adopted for the transport numbers.

10.2.3. Diffusion

According to Fick's law, the flux of electrolyte (2) in a solvent (1) is related to the electrolyte concentration gradient by

$${}_{\omega}\mathbf{J}_2 = -D\ \text{grad}(c_2) \tag{10.15}$$

where D is the diffusion coefficient of the electrolyte measured in the Fick reference system, which is the mean volume velocity, ω, of the system. Unavoidably, a gradient of electrolyte concentration generates a gradient of solvent concentration, leading to a flux of solvent. However, the fluxes of the solution components are related by $\sum_i V_{i\omega} \mathbf{J}_i = 0$, with V_i being the partial molar volume of the i component of the solution. Thus, in binary electrolyte solutions, only the flux of electrolyte is independent, while the flux of solvent in opposite direction is determined by the solute flux.

The binary diffusion coefficient of the electrolyte, D, can be expressed in terms of the diffusion coefficients of the ionic species (Cussler, 1997)

$$D = \frac{|z_+| + |z_-|}{|z_-|/D_- + |z_+|/D_+}. \tag{10.16}$$

The diffusion coefficient is concentration-dependent and its value at infinite dilution is the tracer diffusion coefficient D^0.

For a system of N components the generalized Fick's law:

$${}_\omega\mathbf{J}_i = -\sum_{k=2}^{N} D_{ik}\ \mathrm{grad}(c_k) \tag{10.17}$$

describes the $N-1$ (2,3,…,n) fluxes of the independent components (solvent flow ${}_\omega\mathbf{J}_1$ is the dependent flux). The multicomponent diffusion coefficient D_{ik} gives the flow of solute i produced by the gradient of concentration of solute k. There are $(N-1)^2$ of these coefficients, for instance a ternary system formed by two electrolytes (2,3) in water (1) has four ternary diffusion coefficients: D_{22}, D_{23}, D_{32} and D_{33}. The main diffusion coefficients D_{ii} are positive and usually larger than the cross diffusion coefficients D_{ik}, which could have negative values.

The driving forces for diffusion in the Onsager formalism are not the concentration gradients, but the chemical potential gradients. Thus, for a multicomponent system of N species, the fluxes in the Hittorf reference system are

$${}_1\mathbf{J}_i = -\sum_{j=2}^{N} a_{ij}(\mathrm{grad}\ \mu_j)_{p,T} = -\sum_{j=2}^{N}\sum_{l=2}^{N} a_{ij}\left(\frac{\partial \mu_j}{\partial c_l}\right)_{p,T,c_{k\neq i}} \mathrm{grad}\ c_l. \tag{10.18}$$

The relationship between the diffusion coefficients and the Onsager coefficients, including the change from the Fick to the Hittorf reference systems is given by (Haase, 1990)

$$\sum_{j=2}^{N} a_{ij}\frac{\partial \mu_j}{\partial c_l} = \sum_{k=2}^{N}\left(\delta_{ik} + \frac{c_i V_k}{c_1 V_1}\right)D_{kl} \qquad (i,l = 2,3,\ldots,N) \tag{10.19}$$

where δ_{ij} is the Kronecker delta ($\delta_{ij} = 1$ for $i = j$, $\delta_{ij} = 10$ for $i \neq j$). By resorting to the ORR it is possible to demonstrate that of the $(N-1)^2$ diffusion coefficients, only $N(N-1)/2$ are independent. Thus, for a ternary system formed by two electrolytes in water, there are three independent diffusion coefficients.

As an alternative to Fick's law (Eq. 10.17), the fluxes of species can be related to chemical potential gradients using the Stefan–Maxwell formalism, *i.e.*,

$$-x_i\nabla\mu_i = \frac{RT}{C}\sum_{j=0}^{N}\left(\frac{x_j J_i - x_i J_j}{a_{ij}}\right) \qquad (i = 1,\ldots,N) \tag{10.20}$$

where the subscript 0 denotes the solvent, x_i is the mole fraction of the ith component and C is the total molarity of solutes. The phenomenological

coefficients a_{ij} can be related (Taylor and Krishna, 1993) to the diffusion coefficients D_{ij}. For some applications, it is advantageous to use the Stefan–Maxwell formalism rather than Fick's law because the phenomenological interaction coefficients a_{ij} show a substantially weaker concentration dependence (Graham and Dranoff, 1982; Pinto and Graham, 1987).

In the case of ionic solutes, the driving force is the gradient of the electrochemical potential, which includes chemical potential and local electrical potential gradients. Thus, for a single, completely dissociated, electrolyte the phenomenological equations are

$$\begin{aligned} {}_1\mathbf{J}_+ = &- a_{++}(\text{grad}\,\mu_+ + z_+F\,\text{grad}\,\phi) \\ &- a_{+-}(\text{grad}\,\mu_- + z_-F\,\text{grad}\,\phi) \end{aligned} \tag{10.21a}$$

$$\begin{aligned} {}_1\mathbf{J}_- = &- a_{-+}(\text{grad}\,\mu_+ + z_+F\,\text{grad}\,\phi) \\ &- a_{--}(\text{grad}\,\mu_- + z_-F\,\text{grad}\,\phi) \end{aligned} \tag{10.21b}$$

where ϕ is the diffusion potential. This local potential, defined by Eq. 10.21a,b, can be calculated from these equations by resorting to the zero total current condition ($z_{+1}\mathbf{J}_+ + z_{-1}\mathbf{J}_- = 0$). The diffusion potential is due to the different mobilities of cations and anions moving in the same direction as a consequence of the concentration gradient; it retards the more rapid small ions and accelerates the slower large ions making their velocities equal due to the electric neutrality condition.

The final expression for the diffusion coefficient, obtained by assuming complete dissociation ($\nu_1\mathbf{J}_2 = {}_1\mathbf{J}_+ + {}_1\mathbf{J}_-$) is (Haase, 1990):

$$D = \frac{q^2\nu RT}{c_2}\left(\frac{a_{++}a_{--} - a_{+-}^2}{z_+^2 a_{++} + 2z_+z_-a_{+-} + z_-^2 a_{--}}\right)\left[1 + m\left(\frac{\partial \ln \gamma_\pm}{\partial m}\right)_{T,p}\right] \tag{10.22}$$

where m is the molality, $\gamma_\pm$ the mean activity coefficient of the electrolyte and $q = z_+/\nu_- = z_-/\nu_+$ is a constant. The term in brackets represent a thermodynamic factor in the diffusion.

10.2.4. Limiting Laws

In very dilute solutions where the ion–ion interactions can be neglected, the cross coefficient a_{+-} is zero and we obtain the following limiting expressions

$$\lambda_i^0 = \frac{a_{ii}z_iF^2}{\nu_i c_2} \tag{10.23}$$

$$D^0 = \frac{RT}{F^2}\left(\frac{1}{z_+} + \frac{1}{|z_-|}\right)\left(\frac{\lambda_+^0\lambda_-^0}{(\lambda_+^0 + \lambda_-^0)}\right). \tag{10.24}$$

The last equation, known as the Nernst–Hartley limiting law, has been used to calculate tracer diffusion coefficients from measured limiting ionic conductivities.

According to the stochastic approach (Berry *et al.*, 2000), the movement of ions in dense phases is described by a friction coefficient, ζ, which is independent of the driving force (concentration or potential gradient) and is related to the ion diffusion coefficient ($D_i = RT/\zeta_i$) and to the ion mobility ($u_i = z_iF/\zeta_i$). The common friction coefficient for both types of transport processes leads to the well-known Nernst–Einstein relationship between diffusion and mobility of ionic solutes at infinite dilution:

$$\lambda_i^0 = \frac{z_i F^2}{RT} D_i^0. \tag{10.25}$$

10.2.5. Viscosity

In a continuum fluid system, the shear pressure $\mathbf{p}_{xy}$ (the force exerted per unit area to maintain a flow in the direction x with a velocity gradient $\partial v/\partial y$ in the transverse direction y) is given by Poiseuille's law (see Table 10.1 and Chapter 1).

The forces responsible for viscous friction in pure water are the interactions between water molecules. The presence of ions in the system modifies that friction by introducing solvent–ion and ion–ion interactions, which could increase or decrease friction, depending on the ion characteristics and concentration.

There is only one transport coefficient describing the viscous flow of an electrolyte mixture, independent of the number of species in solution, and the limiting value of this coefficient at zero concentration of electrolyte is the viscosity of pure water. The change of water viscosity with temperature and pressure has been discussed in Chapter 1.

As we will see later, this coefficient related to the momentum transport in the fluid is closely related to the mass and charge transport coefficients.

10.2.6. Thermal Conductivity

The thermal conductivity is the coefficient that quantifies the heat transport through a system. It is defined by Fourier's law (see Table 10.1 and Chapter 1). As with viscosity, the thermal conductivity of an aqueous solution is a single coefficient, independent of the number of species in solution, and its limiting value at zero concentration of electrolyte is the thermal conductivity of pure water.

Unlike the case of viscosity, there is no direct relationship between the thermal conductivity and the mass and charge transport coefficients, except in complex processes taking place under non-isothermal conditions that will not be treated in this work. Nevertheless, water and aqueous electrolyte solutions are extensively used as coolant fluids in a number of industrial processes and the knowledge of

the behavior of thermal conductivity with concentration and state parameters is of major interest.

10.3. Experimental Methods

In this section, the most successful experimental methods and devices used to measure transport properties in high-temperature and -pressure aqueous solutions containing ionic solutes are briefly described, as well as the materials employed for the cells under hydrothermal conditions. The accuracy of the methods, along with the temperature and pressure range covered by each apparatus, is also analyzed.

10.3.1. High-Temperature Electrical Conductivity Cells

Since the pioneering cell of Noyes (1907), a large number of devices have been developed for electrical conductivity measurements under high temperature and pressure conditions; these have been described in detail (Marshall and Frantz, 1987). In this section, we emphasize recent developments that have allowed improvement of the precision of the measurements.

In most of the cells, conductivity measurements were carried out by linear extrapolation of the resistances measured at variable frequencies (commonly from 0.5 to 10 kHz) to infinite frequency, as a function of the inverse of the frequency. The alternative technique, the direct current method, was rarely used.

The design and materials of the conductivity cell must guarantee very small and predictable changes in the cell constant with temperature. The cell constant, a, is usually determined by measuring the resistance, R, of KCl aqueous solutions of known specific conductivity, κ, at 298.15 K (Wu and Koch, 1991)

$$a = \kappa R. \tag{10.26}$$

To estimate the cell constant at higher temperatures, it is common practice to correct for the thermal expansion of the materials used in its construction. Temperature correction factors ranging from 0.1 to 0.4% are reported for different cells used in the temperature range from 298 to 673 K.

A cell developed by Franck (1956) allowed, for the first time, conductivity measurements in supercritical water, at temperatures up to 923 K and pressures up to 250 MPa. This cell design has been used at the Oak Ridge National Laboratory by Marshall and coworkers (Franck *et al.*, 1962; Quist and Marshall, 1968; Frantz and Marshall, 1982, 1984), and later by Palmer and coworkers (Ho *et al.*, 1994; Ho and Palmer, 1996–1998).

The most recent version of the cell (Ho *et al.*, 1994) consists of a platinum–iridium lined high pressure vessel and a thin coaxial platinum wire, insulated by a non-porous sintered Al_2O_3 or Al_2O_3/ZrO_2 tube (for alkaline media). This cell design is not appropriate for measurements at low concentration (lower than

0.001 mol·kg^{-1}) and low densities. For concentrations ranging from 0.001 to 0.1 mol·kg^{-1} and temperatures and pressures up to 873 K and 300 MPa, respectively, Ho *et al.* have reported conductivity measurements of sodium (Ho *et al.*, 1994; Ho and Palmer, 1996), lithium (Ho and Palmer, 1998) and potassium (Ho and Palmer, 1997) chlorides and hydroxides, with a precision better than 0.1%.

In order to perform measurements on aqueous solutions near the critical point of water, a flow-through conductance cell was developed by Wood and coworkers (Zimmerman *et al.*, 1995; Gruszkiewicz and Wood, 1997; Sharygin *et al.*, 2001). The cell was constructed from an 80% platinum–20% rhodium cup (outer electrode), gold soldered to platinum/rhodium tubing used as an inlet tube. On the rim of the cup is an annealed gold washer on top of a sapphire disc insulator, through which is connected the inner electrode, a platinum/rhodium tube. The inner electrode was previously gold-filled at one end, and two small holes on the other end act as the solution outlet. The solution flow sweeps the contaminants dissolving from the sapphire insulator out of the measuring zone and eliminates adsorption effects on the wall of the cell.

A significant improvement in speed and accuracy was achieved by the use of this flow cell. Zimmerman *et al.* (1995) reported conductivity measurements with a precision of about 1% for concentrations as low as 10^{-7} mol·kg^{-1} at a water density of 300 kg·m^{-3} and 0.1% or better for higher concentrations and water densities. The upper pressure limit of this cell is, however, only 28 MPa.

Recently, the Oak Ridge static conductivity cell was modified (Ho *et al.*, 2000a,b, 2001) and converted into a flow-through cell able to operate with high accuracy at densities lower than 0.4 g·cm^{-3}. So far, the maximum temperature achieved is 683 K and the maximum pressure is 33 MPa, but it is expected that the cell could operate up to 873 K and 300 MPa.

The direct-current high temperature flow cell developed by Bianchi *et al.* (1993, 1994) does not possess the precision achieved with the AC flow cells, but it can be preferred for some applications because of its simplicity.

A summary of the aqueous electrolyte systems studied using these modern conductivity cells is shown in Table 10.2.

10.3.2. Determination of Diffusion Coefficients: Electrochemical Methods

The methods for measuring the diffusion coefficient of an electroactive species under conditions of high temperature and pressure involve transient chronoamperometry, steady-state experiments at microelectrodes, and hydrodynamic methods.

Bard and coworkers (McDonald *et al.*, 1986; Flarsheim *et al.*, 1986) have pioneered high-temperature and -pressure devices to permit electrochemical studies in near-critical and supercritical aqueous solutions.

In a very preliminary work (McDonald *et al.*, 1986), a quartz electrochemical cell contained in a steel vessel was used to study the Cu(II)/Cu(I) system in sulfate and chloride solutions up to 573 K. This device was later improved

Table 10.2

Aqueous systems and range of experimental conditions of the electrical conductivity measurements performed using high precision cells

Cell	Electrolyte	m (mol·kg^{-1})	T (K)	p (MPa)	References
AC-static	NaCl	10^{-3}–0.1	373–873	300	Ho *et al.* (1994)
AC-static	NaOH	10^{-3}–0.01	373–873	300	Ho and Palmer (1996)
AC-static	LiCl, LiOH	10^{-3}–0.01	373–873	300	Ho and Palmer (1998))
AC-static	KCl, KOH	10^{-3}–5×10^{-3}	373–873	300	Ho and Palmer (1997)
AC-flow	NaCl, LiCl, NaBr, CsBr	$\approx 10^{-7}$–10^{-3}	579–677	9.8–28	Zimmerman *et al.* (1995)
AC-flow	LiCl, NaCl, NaBr, CsBr	4×10^{-8}–0.013	603–674	15–28	Gruszkiewicz and Wood (1997)
AC-flow	Na_2SO_4	10^{-4}–0.017	300–574	0.1–28	Sharygin *et al.* (2001)
AC-flow	LiCl, NaCl, KCl	10^{-4}–7×10^{-3}	298–683	1–32	Ho *et al.* (2000a)
AC-flow	LiOH, NaOH, KOH	10^{-5}–10^{-3}	323–683	4–32	Ho *et al.* (2000b)
AC-flow	HCl	10^{-5}–10^{-3}	373–683	9–31	Ho *et al.* (2001)
DC-flow	NaOH	$\approx 10^{-3}$	348–423	1.6	Bianchi *et al.* (1994)

(Flarsheim *et al.*, 1986) and the quartz cell replaced by a compact alumina flow cell, which could be heated or cooled quickly and could be recharged with fresh electrolyte solution with an HPLC pump.

In both designs, the diffusion coefficients were obtained from transient chronoamperometric experiments. In this approach, the current density (i)–time (t) response is described by the Cottrell equation (Brett and Brett, 1993):

$$i(t) = nFc\left(\frac{D}{\pi t}\right)^{1/2} \tag{10.27}$$

where n denotes the number of electrons exchanged per species, c is the molar concentration of the electroactive species, and the diffusion coefficient D can be obtained from the slope of a plot of $i(t)$ *vs.* $t^{-1/2}$.

More recently (Liu *et al.*, 1997), the alumina cell was replaced by a titanium cell internally covered with a film of titanium oxide, and the conventional electrode by a microelectrode 25 μm in diameter encapsulated in PbO glass. These modifications allowed the temperature range to be extended to 658 K, and produced a more precise diffusion coefficient from the steady-state diffusion limiting current density, i_{lim}, on the *plateau* region of the sigmoidal shaped wave given by (Brett and Brett, 1993),

$$i_{\text{lim}} = \frac{4nFDc}{\pi r} \tag{10.28}$$

where r is the radius of the microdisk electrode.

Among the hydrodynamic methods, the wall-tube cell and the channel flow cell have shown to be suitable alternatives to the rotating disc electrode (RDE), the last

was rarely employed at high temperature (Wojtowicz and Conway, 1967; McBreen *et al.*, 1984), because of the presence of moving parts in the cell that limits its use to moderate temperatures.

The wall-tube cell developed by Trevani *et al.* (1997) was the first to be applied to the study of aqueous systems at high temperature and pressure. Constructed from titanium and having a working platinum microdisk electrode encapsulated in soda glass as a working electrode, it was used to determine the diffusion coefficients of iodide in $NaHSO_4$ solutions up to 488 K (Trevani *et al.*, 2000).

The limiting current in the *plateau* region of steady-state voltammograms was measured by slowly sweeping back and forth the working electrode potential across the formal potential while the solution is forced to flow and impact on the electrode surface. This limiting current density is related to the diffusion coefficient and the hydrodynamic parameters by (Chin and Tsang, 1978; Trevani *et al.*, 1997)

$$i_{\text{lim}} = \alpha n F D^{2/3} \nu^{-1/6} \left(\frac{H}{d}\right)^{\beta} c^{*} \omega^{1/2} \tag{10.29}$$

where ν is the kinematic viscosity, α and β are two hydrodynamic parameters, ω is related to the flow rate, Q, through $\omega = 4Q/\pi d^3$, H is the tube–electrode distance, d is the tube internal diameter, and the other symbols were defined previously.

Recently, Compton and coworkers (Qiu *et al.*, 2000; Moorcroft *et al.*, 2001) have introduced a high-temperature channel flow cell, in which the working electrode is heated by eddy currents induced by 8 MHz radio frequency (RF) radiation. The very fast local heating and the short residence time of the solution in the high temperature region made it possible to work at temperatures close to the boiling point of the solvent under normal pressure without phase separation. Because the cell operates under 'non-isothermal' conditions, the diffusion coefficients can only be obtained by computer analysis of the experimental results taking into account the mass and heat flow under different conditions.

10.3.3. Diffusion Coefficients: Other Techniques

The Taylor dispersion method (Cussler, 1997) is the most commonly used method for determining molecular diffusion coefficients due to its versatility and experimental simplicity. It is based on the measurement of the dispersion of a sharp pulse of solute injected into a long tube with solvent flowing in laminar flow. For several reasons, this technique is most suited for diffusion measurement at infinite dilution and, so far, few attempts of measurements in sub- and supercritical water have been reported (Goemans *et al.*, 1996).

An optical technique, the laser-induced grating method, was used by Butenhoff *et al.* (1996) to determine diffusion coefficients of concentrated solutions of $NaNO_3$ in supercritical aqueous solutions at temperatures between 673 and 773 K

and pressures in the range 27–100 MPa. This transient method is particularly interesting for measuring short-lived radicals in solution or excited species (Terazima *et al.*, 1995), and it could be used to determine the speed of sound; and thermal and mass diffusivities of supercritical fluids (Kimura *et al.*, 1995).

The method consists of creating a grating by interference of two heating laser pulses of the same wavelength. A sinusoidally temperature and concentration modulated region is created, which in turn generates a spatial modulation of the refractive index in the sample. A third laser beam with a nonabsorbed wavelength is used to read (by Bragg diffraction) the relaxation of the grating due to thermal and mass diffusivity.

The laser-induced grating technique is complementary to the Taylor dispersion method because it performs optimally at higher solute concentration. It has several advantages for measuring diffusivities in hydrothermal solutions because it is a contact-free method which is restricted to a small volume, the temperature and concentration jumps in the sample are small and natural convection is minimized due to the short time scale of the experiment (<5 ms).

A summary of different studies of diffusion in aqueous electrolyte systems is given in Table 10.3.

10.3.4. Viscosity Measurements in Aqueous Solution

The simplest apparatus to measure the viscosity of electrolyte solutions is the rolling-ball viscometer, consisting of an inner tube, a ball and an optical detector. The viscometer is immersed in the thermostat and moved up and down to roll the ball. The viscosity is obtained by measuring the time required to roll the ball through a tube filled with the sample fluid (Sawamura *et al.*, 1990).

The most precise method for measuring the viscosity of corrosive hydrothermal fluids is the oscillating-disk viscometer, used by Dudziak and Franck (1966) to determine the viscosity of pure water up to 833 K and 350 MPa and by Kestin *et al.* (1981a,b) for measuring the viscosity of electrolyte solutions.

A new vibrating-wire viscometer has been developed by Padua *et al.* (1996) that permits the simultaneous measurement of the density and viscosity of fluids at high pressure and temperature. Because the principle of operation is similar to that of the vibrating-tube densimeter, widely used for the measurement of density of ionic aqueous solutions at hydrothermal conditions, the method seems promising for viscosity measurements.

10.3.5. Thermal Conductivity Cells for Conducting Liquids

The parallel-plate cell (Abdulagatov and Magomedov, 1994) and the coaxial cylinder cell (Le Neindre *et al.*, 1973), used to determine the thermal conductivity of pure water by measuring the power transferred between plates maintained at

Table 10.3

Aqueous systems and range of experimental conditions of diffusion measurements performed using electrochemical and optical techniques

Species	Supporting electrolyte	Method and reference	T (K)	p (MPa)
Cu(II)	0.2 M Na_2SO_4	Chronoamperometry, McDonald *et al.* (1986)	295–518	–
Hydroquinone	0.2 M $NaHSO_4$	Chronoamperometry, Flarsheim *et al.* (1986)	298–573	24
Iodide	0.2 M $NaHSO_4$	Chronoamperometry, Flarsheim *et al.* (1986)	298–648	24
Iodide	0.2 M $NaHSO_4$	Microelectrode, Liu *et al.* (1997)	298–658	15–27
Hydroquinone	0.2 M $NaHSO_4$	Microelectrode, Liu *et al.* (1997)	298–658	17.5–27
Fe(II)	0.2 M Na_2SO_4 (pH = 1.5)	Wall-tube electrode, Trevani *et al.* (1997)	306–393	5
Fe(III)	0.2 M Na_2SO_4 (pH = 1.5)	Wall-tube electrode, Trevani *et al.* (1997)	306–393	5
Iodide	0.2 M $NaHSO_4$	Wall-tube electrode, Trevani *et al.* (2000)	291–589	5
$Fe(CN)_6^{4-}$	0.1 M KCl	RF channel cell, Moorcroft *et al.* (2001)	293–348	–
$Ru(NH_3)_6^{3+}$	0.1 M KCl	RF channel cell, Moorcroft *et al.* (2001)	293–348	–
Hydroquinone	0.1 M KCl (pH 1.7 and 6.6)	RF channel cell, Moorcroft *et al.* (2001)	293–348	–
Tetramethyl phenylenediamine	0.1 M KCl	RF channel cell, Moorcroft *et al.* (2001)	293–348	–
Dimethyl phenylenediamine	0.1 M KCl	RF channel cell, Moorcroft *et al.* (2001)	293–348	–
$NaNO_3$	–	Laser-induced grating, Butenhoff *et al.* (1996)	673–773	27–100

a known gradient temperature, have been used for measurements in high-temperature aqueous salt environments.

Corrosion problems limit the accuracy of these measurements and more precise determination of the thermal conductivity of electrolyte solutions can be achieved with the hot-wire method (Baruël, 1973). In this case a thin platinum wire, surrounded by the liquid sample, is heated by circulating a known current through it. The thermal conductivity is calculated from the steady-state temperature increase of the wire, which is measured by sensing its electrical resistance.

The method was later modified to use a transient current to avoid convective problems and increase the accuracy. It is known as the transient hot-wire method and can be used even in acid and salt solutions with an electrically uninsulated wire (Baruël, 1973). Dietz *et al.* (1981) modified the method by using alternating

current in order to avoid polarization problems at the surface of the wire. The accuracy of the AC method was demonstrated by measuring the thermal conductivity of water up to 523 K and 350 MPa.

For electrolyte solutions, several authors have used the transient hot-wire method with a coated wire. Thus, Nagasawa *et al.* (1983) measured the thermal conductivity of NaCl up to 40 MPa and 353 K using a platinum wire insulated with a thin polyester layer. Higher temperatures can be reached by coating the wire, of tantalum for instance, with a layer of its own oxide (Wakeham and Zalaf, 1987).

10.4. Transport Properties of Pure Sub- and Supercritical Water

In Chapter 1, the change of viscosity, thermal and electrical conductivity and self-diffusion with temperature and pressure were discussed for pure water. The presence of ionic solutes generates new diffusion coefficients and also modifies to some extent the transport properties of water in the solution. This chapter deals mainly with those transport properties that are a direct consequence of the presence of ionic solutes, *i.e.*, electrical conductivity and solute diffusion. First, we present a more detailed analysis of the electrical conductivity and self-diffusion of pure water.

10.4.1. The Electrical Conductivity of Water

As mentioned in Chapter 1, the electrical conductivity of pure water as a function of temperature and pressure can be obtained from the known values of K_w, the ion product in molal scale (IAPWS, 1980; Marshall and Franck, 1981) and the limiting conductivities of the hydrogen and hydroxide ions

$$\Lambda_w^0 = c_{H^+}\lambda_{H^+}^0 + c_{OH^-}\lambda_{OH^-}^0 = K_w^{1/2}\rho(\lambda_{H^+}^0 + \lambda_{OH^-}^0). \tag{10.30}$$

Marshall (1987a) described a procedure to estimate $\Lambda^0(H^+, OH^-) = \lambda_{H^+}^0 + \lambda_{OH^-}^0$, over a wide range of temperature and density, based on Eq. 10.10 ($\Lambda^0(H^+, OH^-) = \Lambda^0(HCl) + \Lambda^0(NaOH) - \Lambda^0(NaCl)$) and the known values of the limiting molar conductivity of HCl, NaOH and NaCl extrapolated to infinite dilution using the experimental data by resorting to a reduced-state relationship (Marshall, 1987b):

$$\Lambda^0(\text{salt}) = \Lambda_{00} - S\rho \tag{10.31}$$

where Λ_{00} is the limiting conductivity extrapolated to zero density and S is the slope of the Λ *vs.* density linear plot. Interestingly, the extrapolated limiting conductivity of the H^+ and OH^- ions to zero density (λ_{00}) above 673 K reach the same values as other salt ions.

Although values of the specific conductivity of liquid and supercritical water were reported (Marshall, 1987b) up to 1273 K and 1000 MPa, the reduced-state

Table 10.4
Specific conductivity ($\mu S \cdot cm^{-1}$) of sub- and supercritical water

p (MPa)	298 K	373 K	473 K	573 K	673 K
Saturation	0.0550	0.765	2.99	2.41	–
50	0.0686	0.942	4.08	4.87	1.17
100	0.0836	1.13	5.22	7.80	4.91
200	0.117	1.53	7.65	14.1	14.3
400	0.194	2.45	13.1	28.9	39.2
600	0.291	3.51	19.5	46.5	71.3
800	0.416	4.67	26.7	66.9	110
1000		5.92	34.8	90.2	155

approach is based on experimental data at densities above 0.4 $g \cdot cm^{-3}$; consequently, the predictions below that density are uncertain. Table 10.4 summarizes the predictions up to 673 K and 1000 MPa in the high-density region.

Precise measurements of the electrical conductivity of dilute aqueous NaCl, NaOH and HCl solutions using AC flow and static cells (Table 10.2) allow Marshall's predictions to be tested up to 673 K and 30 MPa. In Fig. 10.2, the limiting molar conductivity $\Lambda^0(H^+, OH^-)$ predicted by the reduced-state approach is plotted at several temperatures between 298 and 673 K as a function of density.

As expected, the agreement with experimental data at 373 and 473 K is very good, but deviations are evident at 573 K even at densities higher than 0.7 $g \cdot cm^{-3}$. The linear relationship between $\Lambda^0(H^+, OH^-)$ and density does not hold at low

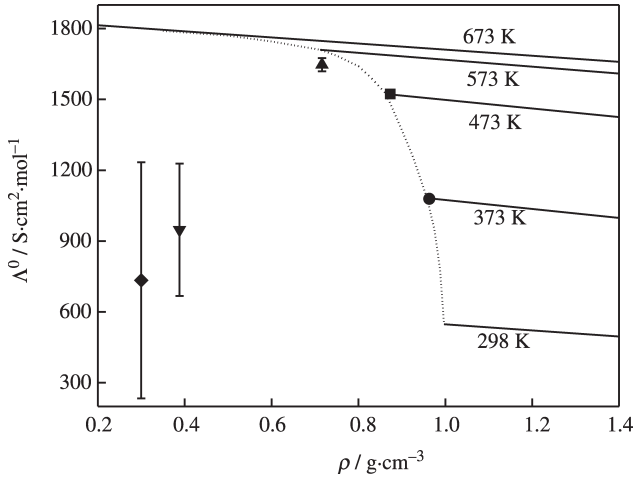

Fig. 10.2. Limiting molar conductivity of pure water as a function of density at several temperatures. Experimental results (Ho *et al.*, 1994, 2001; Ho and Palmer, 1996) 373 K, 0.963 $g \cdot cm^{-3}$ (●); 473 K, 0.873 $g \cdot cm^{-3}$ (●); 573 K, 0.716 $g \cdot cm^{-3}$ (●); 673 K, 0.388 $g \cdot cm^{-3}$ (●); 673 K, 0.301 $g \cdot cm^{-3}$ (◆).

densities, as illustrated by the two points at 673 K shown in Fig. 10.2. Although the uncertainty of these values is very large, the limiting molar conductivity clearly decreases at low densities. These results clearly show that the simple reduced-state approach is unable to describe the electrical conductivity of pure water in the supercritical low-density region. Later we will analyze this point in detail.

It is obvious that the presence of ions will increase the electrical conductivity, but the contribution of H^+ and OH^- ions, that is of the solvent itself, to the total conductivity can be estimated from Eq. 10.30 by replacing the thermodynamic ion product constant K_w by the apparent dissociation quotient $Q_w = K_w a_w/(\gamma_{H^+}\gamma_{OH^-})$, whose value as a function of temperature, pressure and ionic strength has been reported in the literature (Sweeton *et al.*, 1974; Becker and Bilal, 1985).

10.4.2. Self-Diffusion of Water

The self-diffusion coefficient of sub- and supercritical water was discussed in Chapter 1. References were given to recommended values of self-diffusion of liquid water and also to the results by Lamb *et al.* (1981) for compressed supercritical water using the NMR spin-echo technique.

It is interesting to note here that the self-diffusion coefficient of supercritical water was recently determined by Parrinello and coworkers (Boero *et al.*, 2001) using a first-principles molecular dynamics technique. At 673 K these authors found that $D_w = (46.2 \pm 0.6) \times 10^{-5}$ cm^2·s^{-1} at density 0.73 g·cm^{-3} and $D_w = (103.5 \pm 2.1) \times 10^{-5}$ cm^2·s^{-1} at density 0.32 g·cm^{-3}, which agrees rather well with the values reported by Lamb *et al.* (1981).

10.5. Temperature and Pressure Dependence of Ion Limiting Conductivities and Self-Diffusion Coefficients

In a previous section, we analyzed the relation between the friction and the transport coefficients. The simplest friction model is the hydrodynamic Stokes model where the viscous friction ζ_v on a spherical object of radius r moving through a continuum solvent of viscosity η_0 is given by

$$\zeta_v = A\pi r\eta_0. \tag{10.32}$$

A is a constant that depends on the boundary conditions (four for slip and six for stick conditions, respectively). By using this expression for friction, it is possible to obtain expressions for the limiting ionic conductivity:

$$\lambda_i^0 = \frac{z^2 eF}{A\pi r\eta_0} \tag{10.33}$$

known as the Nernst–Einstein (NE) equation, and for the limiting diffusion coefficient

$$D_i^0 = \frac{kT}{A\pi r\eta_0} \tag{10.34}$$

known as the Stokes–Einstein equation (SE).

According to Eq. 10.33, a plot of the Walden product, $\lambda_i^0\eta_0$ *vs.* r^{-1} should yield a straight line for all ions in a given solvent such as water. However, the experimental data show that for the smaller ions the Walden product is lower than that predicted by the NE equation when the crystallographic radii are used for the ions. For this reason, a number of models that account for the interaction of the ion with the dipolar environment have been developed.

10.5.1. Continuum and Molecular Models

In continuum models, the solvent is considered as a medium whose molecular nature is not important, and the friction on the ion is enhanced as its motion disturbs the solvent's equilibrium polarization. The excess of friction of an ion over that predicted by the Stokes–Einstein relation is ascribed to this effect, called dielectric friction. The theory of Zwanzig (1970) leads to the following result for the dielectric friction:

$$\zeta_D = C\frac{(ze)^2(\varepsilon_0 - \varepsilon_\infty)\tau_D}{\varepsilon_0(2\varepsilon_0 + 1)r^3} \tag{10.35}$$

where $C = 3/4$ for slip and $C = 3/8$ for stick conditions, ε_0 and ε_∞ are the static and infinite-frequency dielectric constant of the solvent, respectively, and τ_D is the Debye dielectric relaxation time.

Hubbard and Onsager (1977) developed the most complete continuum theory for ionic friction by solving the Navier–Stokes hydrodynamic equations. In their model, the dielectric friction does not become infinite when the ionic radius tends to zero as predicted by Zwanzig, but it reaches a constant value that depends on the viscosity and dielectric parameters of the solvent. The simplest version of the Hubbard–Onsager theory was formulated by Wolynes (1980) starting with the following expression for the total friction of a moving ion of radius R in a continuum fluid having a distance-dependent viscosity:

$$\frac{1}{\zeta} = \int_R^\infty \frac{dr}{4\pi r^2\eta(r)} \tag{10.36}$$

where the viscosity is given by:

$$\eta(r) = \eta_0\left(1 + \frac{e^2(\varepsilon_0 - \varepsilon_\infty)\tau_D}{16\pi\eta_0\varepsilon_0^2 r^4}\right). \tag{10.37}$$

Xiao and Wood (2000) improved the agreement of the dielectric friction theory with experiment by utilizing a compressible continuum (CC) model (Wood *et al.*, 1994), which describes the change in the solvent density and viscosity as a function of the distance from the ion. In the CC model, the viscosity $\eta(r)$ in Eq. 10.36 is given by a term that accounts for the electrostriction (density enhancement due to electric field) and an electroviscous effect (viscosity enhancement by the electric field). With one adjustable parameter, the radius R_w of the water molecule, this model quantitatively represents limiting conductivities for high densities, but deviates from experimental data for densities below ca. 0.5 g·cm^{-3}. The model predicts the decrease of Walden product with solvent density and the linear relationship between Λ^0 and density at $\rho > 0.5$ g·cm^{-3}, but it fails to predict the large temperature dependence of Λ^0 at $\rho < 0.5$ g·cm^{-3}, as shown for NaCl in Fig. 10.3a.

Fig. 10.3b shows the predictions of the continuum models for the Walden product as a function of the ion radius. If τ_D in the Zwanzig and Hubbard–Onsager theories is calculated with the Debye–Einstein–Stokes equation, it is possible to fit the experimental data at a single temperature by adjusting R_w. Thus, the best fit for the CC model is for $R_w = 0.166$ nm, while a value of 0.22 nm is needed to fit the data with the Hubbard–Onsager theory. In general, this theory underestimates the dielectric friction of small ions, leading to high limiting conductivities for reasonable values of R_w.

The effect of pressure on the dielectric friction has been studied experimentally by Nakahara *et al.* (1982) at 298 K. The Hubbard–Onsager

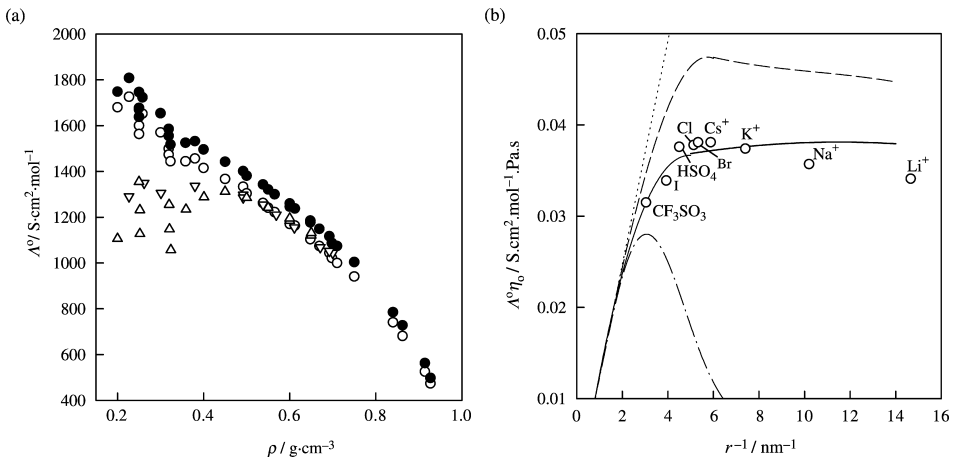

Fig. 10.3. (a) Limiting molar conductivity of NaCl as a function of density at several temperatures from 413 to 673 K: CC model with $R_w = 0.14$ nm (●), and $R_w = 0.166$ nm (●); experimental data: (▽) Zimmerman *et al.*, 1995; (●) Gruszkiewicz and Wood, 1997. (b) Walden product for several ions at 656 K and 28 MPa ($\rho = 0.493$ g·cm^{-3}): dotted line, Stokes' law; dashed line, Hubbard–Onsager theory; dot-dashed line, Zwanzig theory; solid line, CC model ($R_w = 0.166$ nm) (Xiao and Wood, 2000).

theory predicts a decrease of the dielectric friction with pressure, but the experimental results up to 200 MPa show that this is true for the small Li^+ ion, while the larger ions, such as K^+ and Cs^+, show a small increase of the dielectric friction with pressure.

A more elaborate semicontinuum model (Balbuena *et al.*, 1998) used molecular dynamics simulation to determine the water rotational reorientation times in the first coordination shell, which is incorporated into the hydrodynamic Eq. 10.36 for the ionic friction coefficient. Despite this potential improvement in the calculation of the local viscosity around the ions, the model predicts that the limiting conductivity increases approximately linearly with decreasing solvent density, in disagreement with the more recent experimental studies which suggest a decrease in the ionic mobility at low densities.

It is clear that the limitations of the continuum models in explaining the limiting transport properties of ions in water are due to the lack of a molecular description of the ion–water interactions and dynamics. Bagchi and Biswas (1998) have recently shown how a microscopic approach to the friction problem could explain the deviations of ionic mobilities from the Walden product. This molecular model shows how the fast solvation dynamics (in the range of femtoseconds) contribute 60–80% to the total energy relaxation and therefore control the slow mobility of ions in the solvent at high density.

Fig. 10.4 shows the remarkable agreement with experimental data at 298 K obtained with the Bagchi and Biswas model using the available information on the longitudinal components of the ion–dipole correlation functions and

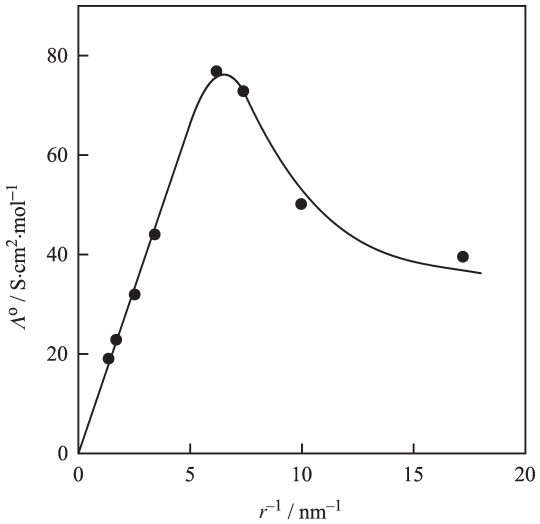

Fig. 10.4. Limiting conductivities of univalent ions in water at 298 K calculated with the Bagchi–Biswas model (Bagchi and Biswas, 1998).

the orientational dynamic structure factor of the pure solvent along with the self-dynamic structure factor of the ion (Biswas and Bagchi, 1998).

Unfortunately, the calculation of the friction at higher temperatures using the molecular model is complex. It requires information on the solvent dynamics and the dynamic structure factor of the ion, which are not available. However, the combination of this molecular model with information obtained from molecular simulation of the ion solvation dynamics (Re and Laría, 1997; Biswas and Bagchi, 1998) could contribute to the development of microscopic models of ionic transport in hydrothermal and supercritical systems.

10.5.2. Empirical Approaches to the Calculation of the Limiting Ion Conductivity

Due to the lack of a precise model for the limiting transport coefficients of ions in water, we will adopt empirical approaches to estimate them as a function of temperature and pressure.

The first attempt to assign limiting conductances for single ions at temperatures up to 673 K was due to Quist and Marshall (1965), who extrapolated transport numbers of KCl and NaCl measured (Smith and Dismukes, 1964) at temperatures up to 398 K. They assumed that the linear relationship between $\log_{10}(t_-/t_+)$ and T^{-1} observed at moderate temperatures is valid over all the temperature range.

A temperature-dependent Walden product was proposed by Smolyakov and Veselova (1975) to predict the ion limiting conductances at temperatures to 473 K:

$$\log_{10}(\lambda^0\eta_0) = A + B/T \tag{10.38}$$

and the values of the parameters A and B were tabulated for several ions.

Marshall (1987b) proposed a reduced-state relationship, Eq. 10.31, to describe the density and temperature dependence of the limiting electrical conductances of salts in aqueous solutions up to 1073 K and 400 MPa. In Eq. 10.31, Λ_{00} is the limiting conductivity extrapolated to zero density and S is the slope of the Λ *vs.* density linear plot. Marshall (1987a) noted that, at all temperatures, these linear plots intersect the density axis at a common value ρ_h. Thus, the slopes can be calculated as $S = -\Lambda_{00}/\rho_h$. By assuming that the zero-density transport numbers of Na^+ and Cl^- are equal over all the temperature range (that is, $\lambda_{00}(Na^+) = \lambda_{00}(Cl^-) = 0.5\Lambda_{00}(NaCl)$), he reported the parameters λ_{00} and ρ_h for several ions up to 673 K.

Other approaches for limiting ion conductivities are based on transport–entropy correlations. Oelkers and Helgeson (1988) described the limiting ionic conductivity or self-diffusion coefficients of ions by an Arrhenius equation of the form

$$\lambda^0 = A_\lambda \exp\left(-\frac{E_\lambda}{RT}\right). \tag{10.39}$$

Based on a correlation between the ionic conductivity and the standard partial molar entropy of the ions, S_i^0, valid to at least 573 K and saturation pressure:

$$\lambda_i^0 = a_i + b_i S_i^0 \tag{10.40}$$

they derived expressions for λ^0 and D^0 of 30 ions at temperatures up to 1273 K and pressures up to 500 MPa. The empirical equations have several adjustable parameters, which account for the temperature and pressure dependence of the activation energy and the coefficients in Eq. 10.40. Therefore, the predictive value of this approach relies on the accuracy of the experimental values of the limiting electrical conductivities reported until the end of the 1980s.

Anderko and Lencka (1997) used Eq. 10.38 with a B coefficient estimated by:

$$\frac{B}{|z|} = a + b\Delta S_{str}^0 + c(\Delta S_{str}^0)^2 \tag{10.41}$$

where ΔS_{str}^0 is the structural entropy of the ion at 298 K, calculated as the difference between the hydration entropy and the Born contribution; also, a constant nonstructural, nonelectrostatic contribution of $-80\ \text{J·mol}^{-1}\text{·K}^{-1}$ is subtracted from the hydration entropy to obtain the structural component. The correlation expressed by Eq. 10.41 depends on the type of ion–solvent interactions in such a way that the parameters a, b and c have common values for all structure-breaking ions ($\Delta S_{str}^0 > -100\ \text{J·mol}^{-1}\text{·K}^{-1}$) and for hydrophobic structure-making ions ($\Delta S_{str}^0 < -100\ \text{J·mol}^{-1}\text{·K}^{-1}$). For strongly electrostrictive structure-making ions (*i.e.*, those that strongly attract water molecules because of their charge and small radius), $B = 0$.

To illustrate the behavior of these models, Fig. 10.5 compares the limiting conductivities of NaCl obtained from the Oelkers and Helgeson (1988), Marshall (1987b) and Smolyakov and Veselova (1975) models with experimental data along the saturation line and outside the saturation region. Outside the saturation region, the recent data of Ho *et al.* (1994, 2000a) and Gruszkiewicz and Wood (1997) were used. It should be noted that these data were not used for regressing the parameters of these models and, therefore, they provide a stringent test of the models. As shown in Fig. 10.5, all three models correctly reproduce the limiting conductivities along the saturation line. The Smolyakov–Veselova model is not appropriate for computing the conductivities away from the saturation line because it does not include any density dependence. The main advantage of this model is its suitability for predicting the temperature dependence of the limiting conductivity along the saturation line using only one experimental point at room temperature and a correlation with the structural entropy (Eq. 10.41). The Marshall and Oelkers–Helgeson models include the density effects either directly (Marshall, 1987b) or through pressure (Oelkers and Helgeson, 1988). For densities above ca. 0.5 g·cm^{-3}, both these models reproduce the new experimental data with reasonable accuracy. However, a significant disagreement with the data is observed for lower densities, mainly in the supercritical region. Here, the Marshall

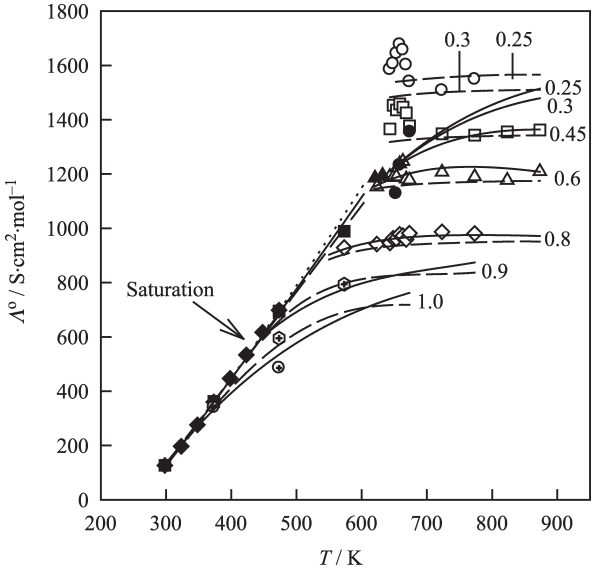

Fig. 10.5. Calculated and experimental limiting conductivities of NaCl as a function of temperature and density. Experimental data from: Smolyakov, 1969 (◆) and Quist and Marshall, 1965 (●) at saturation; Ho *et al.*, 1994, (○) 1 g·cm^{-3}, (○) 0.9 g·cm^{-3}, (◇) 0.8 g·cm^{-3}, (△) 0.6 g·cm^{-3}, (●) 0.45 g·cm^{-3}, (○) 0.3 g·cm^{-3}; Gruszkiewicz and Wood, 1997 (●), 0.6 g·cm^{-3}, (●) 0.25 g·cm^{-3}. The lines show the results calculated using the models of Marshall (1987b), dashed lines; Oelkers and Helgeson (1988), solid lines; and Smolyakov and Veselova (1975), dotted line. The isochors calculated from the models of Marshall (1987b) and Oelkers and Helgeson (1988) are marked with the corresponding values of density.

(1987b) and Oelkers and Helgeson (1988) models show substantially different behavior. At low densities, the data of Ho *et al.* (1994) are in better, although only qualitative, agreement with the model of Marshall (1987b). At the lowest density for which data are available (0.25 g·cm^{-3}), the data of Gruszkiewicz and Wood (1997) seem to agree better, but only qualitatively, with the Oelkers and Helgeson (1988) model.

At this point, it is clear that one should decide between two clearly different behaviors of the limiting conductivity of ions in the low-density region ($\rho < 0.5$ g·cm^{-3}). One is a linear increase of Λ^0 with decreasing solvent density, as suggested by the experimental data from the ORNL group (Ho *et al.*, 1994; Ho and Palmer, 1997, 1998) and one semiempirical model (Marshall, 1987b) and the second is that Λ^0 reaches a *plateau* or even goes through a maximum and then decreases as the solvent density decreases, as can be concluded from the precise measurements on very dilute solutions by Wood and coworkers (Zimmerman *et al.*, 1995; Gruszkiewicz and Wood, 1997).

This dilemma was resolved by the results of molecular simulations and by the very comprehensive analysis by Nakahara and co-workers (Ibuki *et al.*, 2000) of the available data for the limiting conductivity of alkali chlorides in supercritical

water. They concluded that the behavior of Λ^0 is similar for all the salts, and that the ionic mobility reaches a plateau or decreases with decreasing solvent density, as experimentally shown by Wood and co-workers (Zimmerman *et al.*, 1995; Gruszkiewicz and Wood, 1997). The apparent linear increase of Λ^0 with decreasing solvent density reported by the ORNL group was the result of fitting the conductivity data outside the concentration range where the conductivity equations are valid. By limiting the data analysis to concentrations within the correct range, they obtained extrapolated Λ^0 values having the same density dependence reported by Wood and coworkers, even when very low concentrations were not used in the conductivity measurements.

The CC model by Xiao and Wood (2000) also predicts a decreasing limiting conductivity with decreasing solvent density for NaCl down to 0.2 g·cm^{-3}, although the calculated values are 30% higher than the experimental ones.

10.5.3. Molecular Dynamics Simulation of the Limiting Transport Properties

The experimental difficulties of determining transport coefficients in aqueous solutions in the high temperature and supercritical region have encouraged the use of molecular simulation techniques.

Most simulations in aqueous systems use discrete simple point charge models (SPC and SPC/E) for the solvent (Berendsen *et al.*, 1987). The diffusion coefficient of each ion is calculated from the mean-square displacement or from the velocity autocorrelation function (Hansen and McDonald, 1976). The limiting ionic conductivity is calculated from the diffusion coefficient at infinite dilution using the Nernst–Einstein equation (Eq. 10.25).

The number of water molecules used in the simulation limits the concentration of salt of the simulated system. Thus, simulations with one cation and one anion in 215 water molecules are often considered infinite dilution.

Simulation of the diffusion coefficients and limiting conductivity of NaCl (Lee *et al.*, 1998) and LiCl, NaBr, CsBr (Lee and Cummings, 2000) in supercritical water at 673 K and densities between 0.22 and 0.74 g·cm^{-3} have been performed. The results show a clear change of slope from the linear dependence of limiting conductivity proposed by Marshall (Eq. 10.31) at densities below 0.5 g·cm^{-3}, as found experimentally by Zimmerman *et al.* (1995). For these salts, a maximum or a plateau is observed at densities close to 0.3 g·cm^{-3}, as shown in Fig. 10.6, in good agreement with the experimental results. The poor agreement in the case of LiCl is probably due to an underestimation of the mobility of the Li^+ ion, which exhibits a linear dependence of limiting conductivity on the water density.

It is concluded that the number of hydration water molecules around ions dominates the behavior of the limiting conductivity in the high-density region,

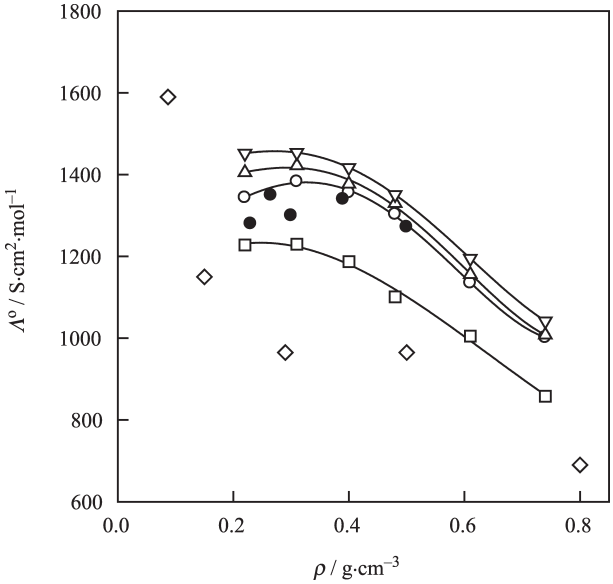

Fig. 10.6. Limiting conductivities of several electrolytes at 673 K as a function of water density. Molecular dynamics simulation (Lee *et al.*, 1998; Lee and Cummings, 2000): (●) NaCl; (△) NaBr; (▽) CsBr; (●) LiCl; (◇) NaCl, molecular dynamics simulation (Hyun *et al.*, 2001). Experimental results for NaCl (●) at 656–677 K (Zimmerman *et al.*, 1995).

while the magnitude of the ion–water interaction, measured by the potential energy per hydration water molecule, dominates in the low-density region.

Koneshan and Rasaiah (2000) performed molecular dynamics simulations of the diffusion of NaCl at 683 K and solvent densities 0.35 and 0.175 g·cm^{-3} at infinite dilution (1 Na^+ and 1 Cl^- ion in 215 water molecules), 0.5 molal (10 Na^+ and 10 Cl^- ions in 1110 water molecules) and 1 molal (10 Na^+ and 10 Cl^- ions in 555 water molecules). The diffusion coefficients at infinite dilution do not agree with those reported by Lee *et al.* (1998), and increase monotonically with decreasing solvent density, but the simulation gives insight into the structure of the solution, revealing that in the concentrated solutions the ion pairing is significant. Thus, small clusters containing Na^+ and Cl^- ions are observed at 0.5 molal while in the 1 molal solution the presence of a single cluster of 10 Na^+ and 10 Cl^- ions is observed. The diffusion coefficient of the ions in the 1 molal solution is half its value at infinite dilution and the values for the cation and anion are nearly equal to each other.

A recent molecular simulation of the diffusion of NaCl in supercritical water at 673 K (Hyun *et al.*, 2001) reaches densities as low as 0.1 g·cm^{-3}, exploring a region not accessible experimentally. The limiting conductivities are around 20% less than the experimental values (Fig. 10.6), but they have the same behavior, showing a *plateau* at densities between 0.3 and 0.5 g·cm^{-3}. Interestingly, the limiting conductivity seems to increase at densities lower than 0.2 g·cm^{-3}, which

is attributed to entropic desolvation of the first hydration shell with an increase of the solvent residence times. This view of an increasingly rigid but smaller hydration shell with decreasing solvent density is also supported by the CC model of Xiao and Wood (2000), leading to an increase in the limiting conductivity. This prediction of the models and molecular simulations has not been yet verified experimentally and it is one of the future challenges in this field.

10.5.4. The Limiting Transport Properties of Complex and Large Ions

In most practical applications, complex species such as metal–halide or metal–hydroxide complexes play an important role. At the same time, very little experimental information is available about the limiting conductivities of complexes. An estimation of the limiting ionic conductivities of ions formed by association of ions of unsymmetrical electrolytes, such as $CaCl^+$ or $NaSO_4^-$, can be obtained from Eq. 10.33; by assuming (Anderko and Lencka, 1997) that the volume of the complex ions is equal to the sum of the volume of the n constituent simple ions:

$$\frac{z_{\text{complex}}}{\lambda^0_{\text{complex}}} = \left[\sum_{i=1}^{n}\left(\frac{z_i}{\lambda_i^0}\right)^3\right]^{1/3} \tag{10.42}$$

The precision of the electrical conductivity measurements of unsymmetrical electrolytes at high temperatures is not enough to allow validation of this approximation, but it seems to be fairly good (Anderko and Lencka, 1997) for predicting ionic conductivities of complex ions at room temperature.

In addition to the limiting conductivity and diffusivity of ions, it is often of interest to compute the limiting diffusivity of neutral molecules. Here, the diffusivities of species such as oxygen, hydrogen and water are of particular importance. Anderko and Lencka (1998) developed a correlation for computing the diffusivity of neutral molecules as a function of temperature. The mathematical form of this correlation is similar to the Smolyakov–Veselova expression for limiting conductivity (Eq. 10.38).

There is a lack of information on the conductivity of large ions, such as tetraakylammonium cations, and tetraphenylarsonium or PF_6^- anions, in high-temperature aqueous solutions. Because the dielectric friction, given by Zwanzig's theory (Eq. 10.35) or the HO theory (Eqs. 10.36 and 10.37), is predicted to decrease with the increasing ion size, it is expected that the simple hydrodynamic model expressed by Eqs. 10.33 and 10.34 could yield reliable values of the limiting transport coefficients when the radius of the ion is much larger than the radius of the water molecule.

In the case of ions of intermediate size, the limiting conductivity could be estimated from Eqs. 10.35–10.37 using the Debye relaxation times of water measured by Okada *et al.* (1997, 1999) at temperatures and pressures up to 1018 K

and 120 MPa. The Debye relaxation time, τ_D, decreases with solvent density until it reaches a plateau at densities between the critical density and 0.6 g·cm^{-3}. Surprisingly, the experimental value increases with decreasing water density at densities below the critical density. This behavior, which could be used to explain the decreasing limiting conductivity of ions at low densities, could not be reproduced by molecular dynamics simulations (Skaf and Laría, 2000) that yielded very good agreement with experimental data at $\rho > 0.4$ g·cm^{-3}.

10.6. Concentration Dependence of the Transport Coefficients

One of the most important tasks for a full description of the transport properties of ionic solutes in aqueous systems at high temperatures and pressures is the prediction of the effect of the concentration. In this section, we will present some of the theoretical and empirical models used to describe transport coefficients as a function of ion concentration, with special emphasis on the treatment of the ion association effect on these coefficients.

10.6.1. Theories of Conductivity of Electrolyte Solutions

The effect of the concentration on the conductance of an electrolyte in very dilute solutions is simple. It was represented empirically by Kohlrausch and later deduced theoretically by Onsager (1927):

$$\Lambda = \Lambda^0 - Sc^{1/2} \tag{10.43}$$

where S is the limiting-law slope, which in the case of symmetrical electrolytes can be expressed as $S = \alpha\Lambda^0 + \beta$, where α and β are given by:

$$\alpha = \frac{82.046 \times 10^4 z^2}{(\varepsilon T)^{3/2}} \tag{10.44a}$$

$$\beta = \frac{8.2487 z}{\eta(\varepsilon T)^{1/2}} \tag{10.44b}$$

with the units of S being S cm^2·mol$^{-3/2}$·dm$^{3/2}$ (the molar concentration is usually expressed as mol·dm^{-3}) and the water viscosity, η, expressed in Pa·s.

In order to illustrate the change of the limiting slope with temperature and pressure in aqueous solutions, Fig. 10.7 compares the calculated Onsager's limiting slope S of aqueous NaCl in different thermodynamic states.

Eq. 10.43 is a limiting law, obtained when the first-order approximation is used and the electrophoretic and relaxational correction terms are separable. Positive deviations from this behavior are expected in non-associated electrolytes due to

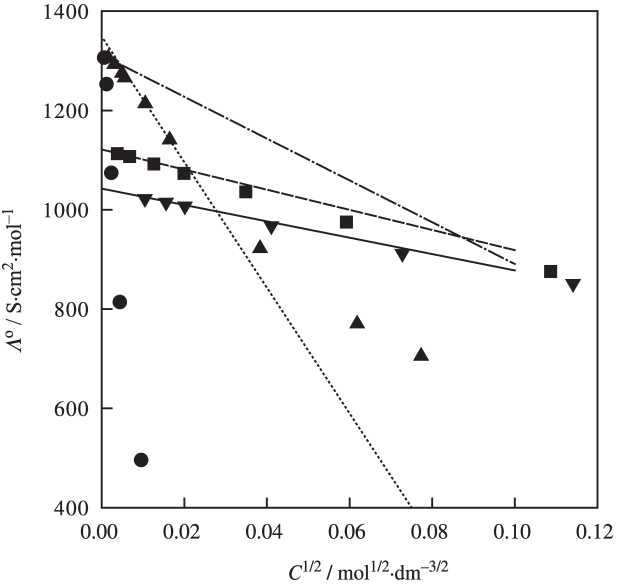

Fig. 10.7. Molar conductivities of NaCl solutions as a function of concentration at different thermodynamic states (Zimmerman *et al.*, 1995; Gruszkiewicz and Wood, 1997). The corresponding limiting Onsager slopes are plotted at each (T, p) : (●●●, ●) $T = 579.4$ K, $p = 9.8$ MPa; (●●●, ●) $T = 603.34$ K, $p = 15.17$ MPa; (●●●●●, ●) $T = 652.8$ K, $p = 24.81$ MPa; (●●●●●●●●●●, ●) $T = 673.1$ K, $p = 28.00$ MPa.

neglected short-range interactions, which make a higher order contribution to conductivity.

There are two strategies for including these higher order contributions in the conductance equation due to Fuoss and Onsager (1957) and Pitts (1953), which have been analyzed in detail in the literature (Fernández-Prini, 1973). Thus, at the end of the 1970s there were several alternative equations to account for the effect of concentration on electrolyte conductances: the Pitts (1953) equation (P), the Fuoss and Hsia (1967) equation (FH) later modified by Fernández-Prini (1969) (FHFP) and valid only for dilute, binary, symmetrical electrolytes, and the Lee and Wheaton (1978) equation (LW) valid for unsymmetrical electrolytes.

The FHFP equation has been widely used to describe the conductance of electrolyte in water and other solvents.

$$\Lambda = \Lambda^0 - SI^{1/2} + EI \ln I + J_1 I - J_2 I^{3/2} \tag{10.45}$$

where I is the ionic strength, defined by $I = 1/2\Sigma z_i c_i$. The coefficients S and E depend only on the charge type of the electrolyte, on the mobility of the ions, on the temperature and on the solvent properties (dielectric constant and viscosity). The J_1 and J_2 coefficients depend also on the minimum distance of approach of free ions, d, (whose meaning is similar to the critical Bjerrum distance although is

not fixed, but is an adjustable parameter). The expressions for J_1 and J_2 depend on the level of approximations used in their derivation (Fernández-Prini, 1973; Justice, 1983). In Table 10.5, we summarize the expressions for the coefficients in Eq. 10.45 for the case of symmetric electrolytes. The expressions for asymmetric electrolytes can be found in the literature (Fernández-Prini and Justice, 1984; Lee and Wheaton, 1978). In Table 10.5, $bd = |z_+z_-|e^2/(\varepsilon kT)$, so that d is equal to the Bjerrum distance for $b = 2$.

The LW equation cannot be expanded in the form of Eq. 10.45 because it contains more complicated functions of I. Like the FHFP equation, it includes a logarithmic term with the same E coefficient, and it depends on the ionic conductivities at infinite dilution and the distance of closest approach, d, of free ions.

More recently, Turq *et al.* (1995) derived a conductivity equation (TBBK) based on the mean spherical approximation (MSA); this can also be applied to unsymmetrical electrolytes. This equation, derived using the Fuoss–Onsager approach, does not contain the logarithmic term when expanded as a function of I. Another difference of the TBBK equation from the classical equations is that it uses as parameters the ionic diameters instead of the distance of closest approach.

A careful comparison of the classical and new theories has been performed recently by Fernández-Prini and coworkers (Bianchi *et al.*, 2000) at 298.15 K. They concluded that, for symmetrical electrolytes in dilute solutions ($\kappa_D a < 0.1$, where $\kappa_D = (8\pi e^2 N_A/\varepsilon kT)^{1/2} I^{1/2}$ is the inverse Debye length) the FHFP equation is superior to the TBBK equation. The TBBK equation is claimed to be precise even at high concentrations, but the deviations from the experimental data are systematic.

A similar comparison by Wood and coworkers (Sharygin *et al.*, 2001) for aqueous NaCl at 623.9 K and 19.79 MPa ($\rho = 0.596$ g·cm^{-3}) indicates that the

Table 10.5

Expressions for the coefficients of the conductivity Eq. 10.45

Coefficient	Term (symmetric electrolyte)
	$E = E_1\Lambda^0 - E_2$
E_1	$2.9425 \times 10^{12}\, z^4/(\varepsilon T)^3$
E_2	$4.3324 \times 10^6\, z^3/\eta(\varepsilon T)^3$
	$J_1 I = 2E_1\{\Delta_1 + \ln(\kappa d/\sqrt{I})\}\Lambda^0 + 2E_2\{\Delta_2 - 2\ln(\kappa d/\sqrt{I})\}$
Δ_1	$(2b^2 + 2b - 1)/b^3 - 0.90735 \quad (\Delta_1 = 2.2824$ for $b = 2)$
Δ_2	$22/3b + 0.01420 \quad (\Delta_2 = 3.6808$ for $b = 2)$
	$J_2 I^{3/2} = 4\kappa bdE_1\Delta_3\Lambda^0 + 2\kappa bdE_2\Delta_4 - 8.2487z\Delta_5 E_2/(\Lambda^0\eta(\varepsilon T)^{1/2})$
Δ_3	$0.9571/b^3 + 1.1187/b^2 + 0.1523/b \quad (\Delta_3 = 0.45546$ for $b = 2)$
Δ_4	$(0.5738b^2 + 7.0572b - 2/3)/b^3 - 0.6461 \quad (\Delta_4 = 1.3218$ for $b = 2)$
Δ	$4/3b - 2.2194 \quad (\Delta_5 = 1.5527$ for $b = 2)$

FHFP equation yields better results than the TBBK equation. Under these conditions, the ion association could not be neglected, even in NaCl, and the conductivity equation includes an ion association term. Thus, the FHFP equation for an associated electrolyte was used:

$$\Lambda = \Lambda^0 - SI^{1/2} + EI \ln I + J_1 I - J_2 I^{3/2} - K_A \Lambda \gamma_{\pm}^2 \alpha c \qquad (10.46)$$

where the coefficients depend on the distance of closest approach, fixed at the Bjerrum distance, d. The NaCl conductivity data were fitted (Sharygin *et al.*, 2001) with the FHFP equation using two (Λ^0 and K_A) or three (Λ^0, K_A and J_2) parameters and the standard deviations were better than those obtained with the TBBK equation. When three parameters were used in the fit, the results became independent of the activity coefficient model used (Bjerrum or MSA).

It is worth noting that at 652.6 K and 22.75 MPa ($\rho = 0.2$ g·cm^{-3}) the performance of both conductivity equations is similar independent of the activity coefficient model. This could be attributed to the poorer accuracy of the experimental data in the low-density region.

The precision of the experimental data is a key issue in choosing an equation to fit the data. Table 10.6 summarizes the values of Λ^0 and K_A obtained by fitting the experimental measurements of the electrical conductivity of aqueous NaCl at temperatures up to 723 K.

The situation for asymmetric electrolytes is more complex, since inconsistencies were observed at 298 K between the association constant obtained from conductivity data and from activity coefficients (Bianchi *et al.*, 2000).

As mentioned previously, the revision by Ibuki *et al.* (2000) of the conductivity data in supercritical water has clarified the general trends of the temperature and density dependence of the limiting conductivities of simple electrolytes. A careful study of the conductivity equations leads to the conclusion that the two-parameter (Λ^0 and K_A) fitting method (FHFP2) provides more reliable results than three-parameter methods (FHFP3) in a moderate concentration range. It was also observed that the FHFP equation 10.46, or the more simple Shedlovsky equation (Harned and Owen, 1950), gives similar fitting results, as shown in Table 10.6 for LiCl solutions at 658 K and $\rho = 0.251$ g·cm^{-3}.

The contribution of the electrophoretic effect to the concentration dependence of the molar conductivity is expected to be lower in supercritical water than in ambient water because of the much smaller viscosity and dielectric constant. Thus, the ratio $\beta/\alpha\Lambda^0$ in Eq. 10.44 decreases from 2.29 at 298 K and 1.0 g·cm^{-3} to 0.62 at 758 K and 0.25 g·cm^{-3}. This is why differences among several conductivity equations vanish at supercritical conditions.

On the other hand, Ibuki *et al.* (2000) have demonstrated that the higher order terms in Eq. 10.46 or similar ones nearly cancel each other at moderate concentration in supercritical water, as can be seen in Table 10.7. This could be the reason for the success of simpler conductivity equations under these conditions.

Table 10.6
Limiting conductivity and association constant of aqueous NaCl and LiCl from conductivity data

c (mol·dm^{-3})	T (K)	ρ (g·cm^{-3})	Fitting equation	Λ^0 (S·cm^2·mol^{-1})	$\log_{10} K_A$	References
NaCl						
(7–700) × 10^{-4}	623.15	0.70	Shedlovsky	1045	No association	Quist and Marshall (1968)
	623.15	0.80		945		
(6–800) × 10^{-4}	623.15	0.65	Shedlovsky	1113 ± 23	1.083	Ho *et al.* (1994)
	623.15	0.80		942 ± 20	0.633	
(3–1300) × 10^{-5}	579.47	0.700	FHFP	1043 ± 1	0.95 ± 0.05	Zimmerman *et al.* (1995)
	601.73	0.692		1052 ± 2	1.05 ± 0.07	
	604.57	0.671		1068 ± 1	1.13 ± 0.04	
(1–1180) × 10^{-5}	603.28	0.650	FHFP	1121 ± 1	1.22 ± 0.03	Gruszkiewicz and Wood (1997)
	616.23	0.650		1132 ± 1	1.25 ± 0.03	
	620.43	0.600		1185 ± 1	1.46 ± 0.02	
(1.5–66) × 10^{-4}	623.9	0.596	FHFP	1191 ± 2	1.49 ± 0.03	Sharygin *et al.* (2001)
	623.9	0.596	TBBK	1184 ± 10	1.37 ± 0.07	
	652.6	0.200	FHFP	1106 ± 30	5.03 ± 0.08	
	652.6	0.200	TBBK	1106 ± 30	5.03 ± 0.08	
LiCl						
(5–244) × 10^{-7}	658.07	0.251	FHFP3	1208 ± 9	4.15 ± 0.02	Gruszkiewicz and Wood (1997)
(5–244) × 10^{-7}	658.07	0.251	Shedlovsky	1203 ± 11	4.13 ± 0.02	Ibuki *et al.* (2000)
	658.07	0.251	FHFP2	1206 ± 8	4.14 ± 0.02	
(1–10) × 10^{-3}	773.15	0.550	Shedlovsky	1219 ± 62	2.06 ± 0.16	Ibuki *et al.* (2000)
	773.15	0.550	FHFP2	1237 ± 64	2.15 ± 0.19	
(3–30) × 10^{-4}	773.15	0.300	Shedlovsky	826 ± 84	3.02 ± 0.18	Ibuki *et al.* (2000)
	773.15	0.300	FHFP2	873 ± 116	3.17 ± 0.20	

K_A in molal standard scale.

Table 10.7

Contribution of the individual terms (in $S \cdot cm^2 \cdot mol^{-1}$) for a modified version by Justice (1983) of Eq. 10.47 for LiCl (Ibuki *et al.*, 2000)

Conditions	c ($mol \cdot dm^{-3}$)	Λ^0	$-S(\alpha c)^{1/2}$	$E\alpha c \log_{10}(\alpha c)$	$J_1 \alpha c$	$-J_2(\alpha c)^{3/2}$	$-\Lambda \alpha c \gamma_{\pm}^2 K_A$
298 K, 1.00 $g \cdot cm^{-3}$	0.030	115.1	−15.1	−0.9	4.9	−0.8	0.0
758 K, 0.251 $g \cdot cm^{-3}$	0.030	1208	−439	−1453	2825	−1275	−830
	0.0024	1208	−209	−402	640	−138	−972
	0.00047	1208	−128	−169	240	−32	−872

It should be noted that the concentration dependence of the molar conductivity in aqueous solutions at temperatures near or above the critical point of water is dominated by the association constant (last term in Eq. 10.46), and consequently negative deviations from the limiting law are expected. Fig. 10.7 shows that an NaCl solution at 579.4 K and 9.8 MPa slightly deviates from the ideal behavior due to its extensive dissociation ($K_A = 8.9$, according to Zimmerman *et al.*, 1995). The association constant increases with temperature following the Arrhenius law and the negative deviations from the limiting law become very large, as can be seen in Fig. 10.7 for NaCl at 673.1 K and 28.0 MPa ($K_A = 1.5 \times 10^4$).

10.6.2. Diffusion in Concentrated Solutions

Prior to discussing the methods for computing the concentration dependence of diffusion in electrolyte solutions, it is necessary to classify the diffusion processes that are of interest in practice. In general, it is necessary to distinguish between self-diffusion (also referred to as intradiffusion) and mutual diffusion (or interdiffusion). Following Mills and Lobo (1989), we use the term 'self-diffusion' to denote three cases, *i.e.*,

1. Diffusion in a pure fluid;
2. Tracer (or single-ion) diffusion, *i.e.*, the diffusion of a tracer species that is chemically equivalent to one of the ions in the solution, but is isotopically different. Since the different isotopes are chemically identical, the tracer diffusion is equivalent to the self-diffusion of the labeled ion in the solution.
3. Diffusion of a species that is not an isotopomer of any other component of the solution, hence is chemically different. In this case, the diffusing species must be present in a trace amount.

On the other hand, the terms mutual- or interdiffusion pertain to the diffusion in a system in which there is a concentration gradient. A significant difference between mutual- and self-diffusion in binary solutions lies in the electroneutrality constraint. In mutual diffusion, the constraint of maintaining electrical neutrality entails that positive and negative ions move along the concentration gradient at the same speed. Therefore, in a binary solution, there is only one mutual diffusion coefficient. In self-diffusion, however, the electrical neutrality constraint does not apply and it is convenient to define the self-diffusion coefficients separately for all species in the solution (*e.g.*, for the cation, anion and solvent molecule in a binary solution). Thus, mutual diffusion coefficients are usually measured for electrolytes as a whole whereas self-diffusion coefficients are obtained for individual species.

There is no simple relationship between self- and mutual diffusion coefficients for systems at finite concentration. Such a relationship is available only at infinite dilution and is given by Eq. 10.16 for the special case of a system consisting of one cation and one anion. Thus, separate computational models are necessary to calculate mutual- and self-diffusion coefficients.

On the molecular level, the difference between mutual- and self-diffusion manifests itself in the relaxation and electrophoretic effects (*cf.* Robinson and Stokes, 1959). The relaxation effect arises from the disturbance of the symmetrical arrangement of ions in the solution as they move. The electrophoretic effect results from the transfer of force, through the solvent, between moving ions. The relaxation effect is important for self-diffusion whereas it vanishes for mutual diffusion in binary solutions. This is because, in mutual diffusion, the positive and negative ions in a binary solution move with the same velocity, thus preserving the symmetry of the ionic atmosphere. In self-diffusion, the tracer ion moves against the background of non-diffusing ions, which disturbs the symmetry of the ion atmosphere and produces the relaxation effect. The electrophoretic effect, on the other hand, can be neglected for self-diffusion whereas it remains significant for mutual diffusion. The electrophoretic effect is negligible for self-diffusion because the concentration of the tracer species can be regarded as infinitesimally low. Thus, quantitative models for self-diffusivity should incorporate only the relaxation effect.

10.6.2.1. Self-Diffusion

As with electrical conductivity, the concentration dependence of self-diffusion has been extensively studied using the methods of statistical mechanics. Onsager (1931a,b, 1945) developed a limiting law using the Debye and Hückel (1924) equilibrium distribution functions. This theory was later extended to multi-component solutions by Onsager and Kim (1957). According to this law, the relaxation effect causes the deviation of the self-diffusion coefficient from its value at infinite dilution, *i.e.*,

$$D_i = D_i^0\left(1 + \frac{\delta k_i}{k_i}\right) \tag{10.47}$$

where $\delta k_i/k_i$ is the relaxation term and is given by

$$\frac{\delta k_i}{k_i} = -\frac{\kappa_D z_i^2 e^2}{3\varepsilon kT}(1 - \sqrt{d}) \tag{10.48}$$

where κ_D is the inverse Debye screening length, defined in Section 10.6.1, z_i is the charge and ε is the dielectric constant. In the simple case of a tracer species 1 in an electrolyte containing ions 2 and 3, the function d takes the form

$$d = \frac{|z_1|}{|z_1| + |z_2|}\left(\frac{|z_2|\lambda_2^0}{|z_1|\lambda_2^0 + |z_2|\lambda_1^0} + \frac{|z_3|\lambda_3^0}{|z_1|\lambda_3^0 + |z_3|\lambda_1^0}\right) \tag{10.49}$$

where λ_i^0 denotes the limiting conductivity of ion i. This model is valid only within the validity range of the Debye–Hückel distribution functions, *i.e.*, for dilute solutions.

More recently, Bernard *et al.* (1992) developed an expression for $\delta k_i/k_i$ for the unrestricted primitive model, *i.e.*, a system of ions with different sizes in a dielectric continuum. This expression was obtained by combining the Onsager continuity equations with equilibrium correlation functions calculated from the MSA theory. This made it possible to extend the range of concentrations for which the model is applicable to approximately 1 M. In the MSA theory, the characteristic parameters are the sizes of ions in the solution. In a related paper, Chhih *et al.* (1994) developed a simplified expression, in which the average size approximation was used for the ionic sizes. The MSA expressions for $\delta k_i/k_i$ are given in the original papers and will not be repeated here. Bernard *et al.* (1992) and Chhih *et al.* (1994) demonstrated that the MSA theory is capable of reproducing experimental data at room temperature up to 1 M for monovalent ions using crystallographic radii as characteristic parameters for ions. Because of a lack of self-diffusion data for relatively concentrated solutions at high temperature, the validity of such predictions at elevated temperatures has not been verified.

Anderko and Lencka (1998) utilized the MSA theory of self-diffusion to develop a model that is applicable to concentrated aqueous electrolyte solutions and, at the same time, can be used for both ionic and nonionic species (*e.g.*, solvent molecules or dissolved gases). For this purpose, they noted that in systems with substantial ionic concentration, the long-range interionic forces are effectively screened to short range by patterns of alternating charges. Then, interionic forces can be combined with all other interparticle forces on the same basis. Thus, all interparticle forces in concentrated solutions can be effectively treated as short-range forces and the solution properties can be calculated by methods similar to those for nonelectrolytes. The alternating charge pattern does not apply to dilute solutions and, therefore, 'nonelectrolyte-type' theories are not necessary in the dilute region. This rationale was used previously (Pitzer, 1980; Pitzer and Simonson, 1986) to develop thermodynamic models by combining a long-range electrostatic interaction term with terms developed for nonelectrolyte solutions. This approach is also applicable to transport properties. In the case of self-diffusion, the composition dependence in concentrated solutions can be represented by the hard-sphere theory, which is applicable to nonelectrolyte solutions. Therefore, Eq. 10.47 can be modified as follows:

$$D_i = D_i^0 \left(\frac{D_i^{\mathrm{HS}}}{D_i^0} \right) \left(1 + \frac{\delta k_i}{k_i} \right) \tag{10.50}$$

where the first term in parentheses denotes the hard-sphere contribution. For binary systems, a closed-form expression for the hard-sphere term was developed by Tham and Gubbins (1971). As with the MSA theory, the hard-sphere term can be computed if the radii of all ions and neutral species are known. To a first approximation, crystallographic radii can be used. For more concentrated

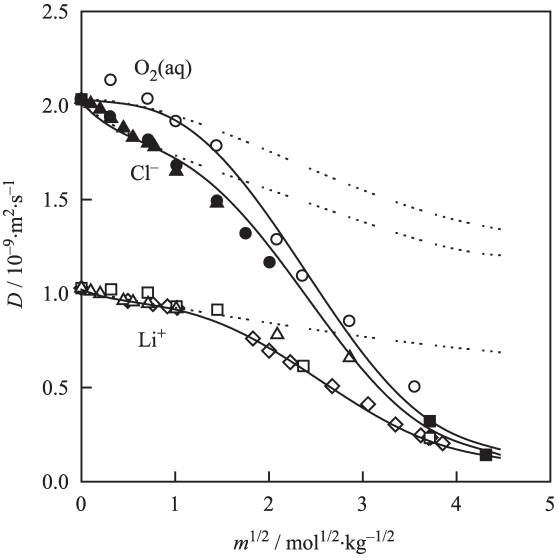

Fig. 10.8. Self-diffusion coefficients for Li^+, Cl^- and O_2 in the system $LiCl + H_2O + O_2$ at 298.15 K. The lines were obtained from a model that combines the relaxation and hard-sphere terms (Eq. 10.50) using crystallographic radii (dashed lines) or effective radii (solid lines). The data for the Li^+ and Cl^- ions were taken from the compilation of Mills and Lobo (1989), pp. 97–110: ◇ — Li^+, Braun and Weingärtner (1988); ● — Li^+, Tanaka and Nomura (1987); △ — Li^+, Turq *et al.* (1971); ● — Cl^-, Mills (1957) and ● — Cl^-, Tanaka and Nomura (1987). The data for O_2 (●) were taken from Ikeuchi *et al.* (1995).

solutions, it is necessary to use effective species radii as described by Anderko and Lencka (1998).

To illustrate the features of this model as well as the general behavior of self-diffusivities as a function of concentration, Fig. 10.8 shows the behavior of diffusing species in the system $LiCl + H_2O + O_2$ at 298 K. Unfortunately, such experimental data are not available at elevated temperatures, so we have to rely on room-temperature data to assess the performance of the model. As shown by the dotted lines in Fig. 10.8, the model can predict the composition dependence up to ca. 1 M using crystallographic radii. Beyond this range, effective radii are necessary. It should be noted that the adjustment of radii is necessary only for ionic species that exist in high concentrations (*e.g.*, effective radii are needed only for Li^+ and Cl^- and not for H_2O or O_2 in the example shown in Fig. 10.8).

Experimental self-diffusion data are relatively abundant for conditions near room temperature. The compilation by Mills and Lobo (1989) provides a comprehensive collection for ions and water molecules in various solutions. These data, however, are in most cases limited to temperatures below 373 K. Thus, it is necessary to rely on model predictions to evaluate the concentration dependence of self-diffusivity at higher temperatures. Such predictions should be reasonable because most of the temperature dependence of self-diffusivity is embedded in

the diffusivity at infinite dilution (D_i^0). Both the relaxation and hard-sphere terms are relatively weakly dependent on temperature. The relaxation term depends on the dielectric constant of the solvent. The hard-sphere term depends on the density of the solution, which can be reasonably computed from a separate model. Also, the effective ionic radii, which determine the composition dependence of both terms for concentrated solutions, are independent of temperature (Anderko and Lencka, 1998), at least within a moderate temperature range, *i.e.*, up to 373 K. This allows the model to provide reasonable estimates at higher temperatures even though the model parameters are determined from data at lower temperatures.

10.6.2.2. Mutual Diffusion

In contrast to self-diffusion, mutual diffusion coefficients must be defined with respect to a certain reference frame. The volume-fixed reference frame defines the flux of diffusing species across a plane fixed so that the total volumes on each side of the plane remain constant. Such a frame is fixed with respect to the measuring apparatus. Other reference frames have been described by Tyrrell and Harris (1984) and will not be discussed here. A general expression for the volume-fixed diffusion coefficient in electrolyte or nonelectrolyte solutions has been derived by Hartley and Crank (1949) for a binary system composed of two components, A and B. In such a system, there is only one mutual diffusion coefficient, D_V, and it is given by

$$D_V = \frac{\partial \ln a_A}{\partial \ln x_A}\left(x_B D_{AB}^0 + x_A D_{BB}^0\right)\frac{\eta_B^0}{\eta} \tag{10.51}$$

where x denotes the mole fraction, η is the viscosity, D_{AB}^0 is the tracer diffusion coefficient of A at infinite dilution in B and D_{BB}^0 is the self-diffusion coefficient of B in B. Because of symmetry, the same value of D_V can be obtained by switching the subscripts A and B. The first two terms can be derived by considering the simultaneous diffusion of the components A and B on the assumption that their partial molar volumes are constant. However, the last term, η_B^0/η, was introduced into Eq. 10.51 on an empirical basis. The empirical effectiveness of this term is a manifestation of the fact that the effects of concentration on both diffusion and viscosity follow the same regularities. Therefore, empirical data (or correlation equations) for viscosity can be utilized to predict the concentration dependence of mutual diffusion. Over wide concentration ranges, it is generally observed that the largest effects on mutual diffusivity are due to the thermodynamic term $\partial \ln a_A/\partial \ln x_A$ and the viscosity correction. Thus, the two most significant terms can be predicted using data for different properties (*i.e.*, viscosity data and vapor pressure or other equilibrium data for the thermodynamic term).

In dilute binary solutions, the concentration dependence of mutual diffusion is primarily due to the electrophoretic effect as discussed above. Onsager and Fuoss

(1932) developed a limiting law for the mutual diffusivity. In concentrated solutions, however, the electrophoretic effect becomes numerically small in comparison to the thermodynamic term.

Wishaw and Stokes (1954) and Robinson and Stokes (1959) utilized the Onsager and Fuoss (1932) treatment of dilute solutions in conjunction with the Hartley and Crank (1949) phenomenological equation to develop a predictive correlation that is valid up to fairly high concentrations. The model was further refined by assuming that the diffusing entity is a hydrated solute rather than bare ions. This assumption introduced another characteristic parameter, the hydration number h. The combined model is given for an $MX-H_2O$ solution by:

$$D_{MX} = (D^0_{MX} + \Delta_1 + \Delta_2)\left(1 + m\frac{\mathrm{d}\ln\gamma}{\mathrm{d}m}\right)(1 - M_w hm)$$
$$\times\left[1 + M_w m\left(\frac{\nu D^0_w}{D^0_{MX}} - h\right)\right]\frac{\eta_0}{\eta} \qquad (10.52)$$

where Δ_1 and Δ_2 are the electrophoretic corrections, the second term in parentheses is the thermodynamic term expressed in terms of molality, D^0_w is the self-diffusion coefficient of pure water, η_0 is the viscosity of pure water, η is the viscosity of the solution and ν is the number of ions that result from the dissociation of the solute. The electrophoretic terms are given, for a binary solution, by

$$\Delta_n = kTA_n\frac{(z_1^n t_2^0 + z_2^n t_1^0)^2}{a^n|z_1 z_2|} \qquad (10.53)$$

where t_i^0 are transference (or transport) numbers at infinite dilution, which can be obtained from ionic limiting conductivities and the coefficients A_n are functions of the dielectric constant and viscosity of the solvent (Robinson and Stokes, 1959; Onsager and Fuoss, 1932). In the original work of Onsager and Fuoss (1932), both electrophoretic corrections Δ_1 and Δ_2 are used. However, Robinson and Stokes (1959) proposed dropping the Δ_2 term for unsymmetrical electrolytes.

Eq. 10.52 has been shown to have good predictive capabilities for concentrations up to several mol $(\mathrm{kg\ H_2O})^{-1}$. Typical deviations are within 1% for concentrations up to 1 molal and 2–3% up to several molal. Other techniques for correlating mutual diffusion coefficients have been reviewed by Tyrrell and Harris (1984) and Horvath (1985).

It should be noted that experimental data on the concentration dependence of mutual diffusion coefficients are available only at room and at moderately elevated temperatures. A comprehensive collection of data published until the late 1980s is provided by Lobo and Quaresma (1989).

For high-temperature systems, model-based estimates are necessary. In particular, Lindsay (1980) used Eq. 10.52 to estimate mutual diffusion coefficients

for NaCl for temperatures up to 673 K. To make these estimates, Lindsay observed that the ratio of limiting diffusivities $D^0_{H_2O}/D^0_{MX}$ and the hydration number h could be assumed to be independent of temperature. Furthermore, Lindsay adjusted the value of h using experimental data at room temperature up to 1 molal. The thermodynamic term could be calculated directly because activity-coefficient data are available for NaCl at high temperatures (Liu and Lindsay, 1971) and it is responsible for most of the strong concentration dependence of the diffusion coefficient observed at high temperature. Viscosity data (Kestin *et al.*, 1981a,b) could be used directly for temperatures up to 423 K and extrapolated to higher temperatures. Fig. 10.9 shows the D_{MX}/D^0_{MX} ratios predicted using Lindsay's approach. As shown in Fig. 10.9, the predicted values are in reasonable agreement with experimental data at room temperature. The agreement could be further improved by fitting the hydration parameter h over the full concentration range. In the absence of high-temperature data, this method can be recommended for estimating mutual diffusion coefficients at elevated temperatures.

10.6.3. Viscosity of Electrolyte Solutions

As with electrical conductivity and diffusivity, the primitive model of long-range electrostatic interactions in dilute electrolyte solutions makes it possible to derive a limiting law for the relative viscosity (*i.e.*, the ratio of the viscosity of the solution

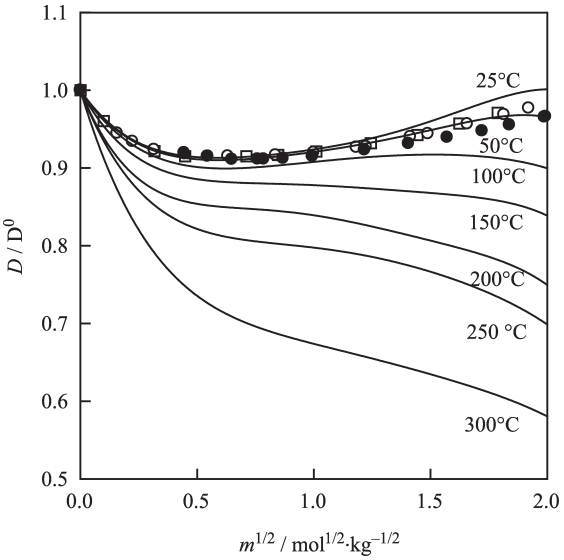

Fig. 10.9. Concentration dependence (in relation to the infinite-dilution value) of mutual diffusion coefficients of NaCl in H_2O calculated using Eq. 10.52 and the procedure developed by Lindsay (1980). The experimental data were taken from the compilation of Lobo and Quaresma (1989): ● — Rard and Miller (1979), 298.15 K; ● — Miller (1966), 298.15 K and ● — Vitagliano (1960), 323.15 K.

to that of the solvent at the same temperature and pressure):

$$\eta_r = \eta/\eta_0 = 1 + AI^{1/2}. \tag{10.54}$$

A general expression for the coefficient A in multicomponent solutions was developed by Onsager and Fuoss (1932):

$$A = a\frac{1}{\eta_0}\left(\frac{2}{\varepsilon T}\right)^{1/2}\left[\left(\sum_{i=1}^{N_I}\frac{\mu_i z_i}{\lambda_i}\right) - 4r\sum_{n=0}^{\infty} c_n s^n\right] \tag{10.55}$$

where a is a constant, ε is the dielectric constant of the solvent, λ_i is the limiting conductivity of ion i, μ_i, r and s are functions of limiting conductivities and c_n are constants. When the λ_i values are in S mol^{-1}·cm^2, I is in mol dm^{-3} and η_0 is in Pa·s, the constant a is 0.364541. This limiting law is valid in the concentration range 0–0.002 molal. Since the viscosity of the solution in this range is not much different from that of the pure solvent, the practical usefulness of this equation is very limited. An important extension of the limiting law to somewhat higher (although still small) concentrations was proposed by Jones and Dole (1929). For multicomponent solutions, the Jones–Dole equation can be written as:

$$\eta_r = 1 + AI^{1/2} + \sum_i c_i B_i \tag{10.56}$$

where B_i are the Jones–Dole coefficients for each individual ion. This equation is typically valid for concentrations up to 0.1 molal, although it may be applicable to higher concentrations for some systems. The B_i coefficients are characteristic for each ion and are additive for electrolytes. The ionic coefficients can be determined from those for individual solutes with the often used convention $B_{K^+} = B_{Cl^-}$. Therefore, the Jones–Dole equation should be treated as an extended limiting law rather than a merely empirical expression. Much attention has been focused in the literature on the relationship between the B_i coefficients and ion–solvent interactions (*cf.* a review by Marcus (1985)). Although it is accepted that the magnitude of the B_i coefficients depends on the structure-making and structure-breaking properties of ions, no general technique is available for predicting the coefficients.

A comprehensive collection of B_i coefficients at room temperature is available in the compilation by Marcus (1997). Therefore, it is more important to predict the temperature dependence of these coefficients than their absolute values. For this purpose, a useful equation was proposed by Out and Los (1980):

$$B = B_E + B_s \exp[-K(T - 273.15)] \tag{10.57}$$

where the parameter K can be assigned a universal value of 0.023. The representation of experimentally determined B coefficients using the Out–Los equation is shown in Fig. 10.10 for selected ions.

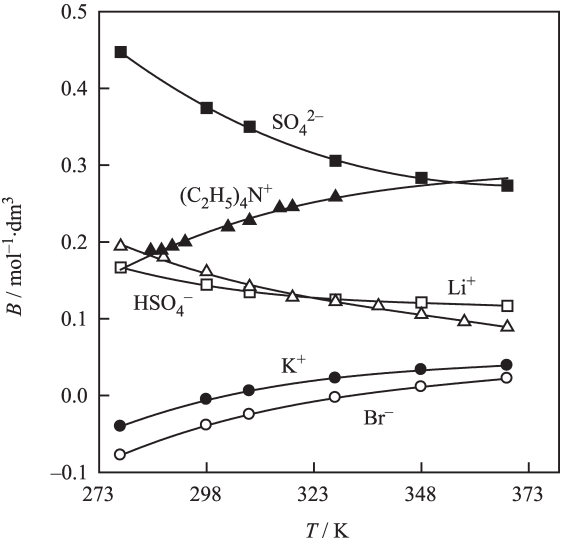

Fig. 10.10. Temperature dependence of the viscosity B coefficients calculated using the Out–Los equation for selected ions.

As shown in Fig. 10.10, the variation with temperature of the B coefficients becomes weaker with rising temperature. Therefore, the Out–Los equation can be used to extrapolate the B coefficients to higher temperatures using experimental data at temperatures below ca. 373 K. Moreover, Lencka *et al.* (1998) developed a technique for predicting the parameter B_s in the Out–Los equation using the entropy of hydration. Using this correlation, the B coefficients can be predicted as a function of temperature using only one experimental point at room temperature (which is the only experimental datum available for most ions).

To compute the viscosity of concentrated solutions, it is necessary to use empirical techniques. Several techniques are available for single-solute systems (Horvath, 1985). A particularly simple equation, known as the Othmer rule (Korosi and Fabuss, 1968), relates the viscosity of a salt solution to that of water, *i.e.*,

$$\ln \eta_r(T, m) = a(m) + b(m) \ln \frac{\eta_{H_2O}(T)}{\eta_{H_2O}(T_{ref})} \tag{10.58}$$

where $a(m)$ and $b(m)$ are empirical (typically, polynomial) functions of molality but not of temperature. The advantage of this equation is its simplicity and capability of correlating viscosity data essentially within experimental uncertainty. Additionally, it performs well when extrapolated to higher temperatures (Lindsay, 1980). However, it does not reduce to the Jones–Dole equation at low concentrations and is not applicable to very concentrated solutions. Thus, this equation is more suitable for the reduction of experimental

data in single-solute systems rather than for modeling the viscosity of more complex solutions.

A more general approach to calculating the viscosity of concentrated solutions is based on extending the Jones–Dole equation. A practical extension for single-solute systems was first proposed by Kaminsky (1957), who added a quadratic term to obtain an equation that is valid for concentrations up to several molal:

$$\eta_r = 1 + Ac^{1/2} + Bc + Dc^2. \tag{10.59}$$

Based on Kaminsky's concept, Lencka *et al.* (1998) developed a general expression for multicomponent systems that is valid up to saturation for most aqueous systems:

$$\eta_r = 1 + AI^{1/2} + \sum_i c_i B_i + \sum_i \sum_j f_i f_j D_{ij} I^2 \tag{10.60}$$

where f_i and f_j are fractions of the ith and jth species, respectively, and D_{ij} is the interaction parameter between i and j. The fractions f_i are defined as modified molar fractions, *i.e.*,

$$f_i = \frac{c_i/l_i}{\sum_k c_k/l_i} \tag{10.61}$$

where the factor l_i is the greater of $|z_i|$ or 1. For concentrated solutions, the parameter D_{ij} in Eq. 10.60 depends on the ionic strength:

$$D_{ij} = d_1 + d_2 I + d_3 \exp(0.08 I^{3/2}) \tag{10.62}$$

where d_1, d_2 and d_3 are empirical parameters. The parameters d_2 and d_3 are required only for systems with a substantial ionic strength (usually above 5 molal). They have a weak temperature dependence, which can be expressed by a simple exponential function:

$$d_i = d_{i,0} \exp\left[d_{i,1}(T - 273.15)\right]. \tag{10.63}$$

Eqs. 10.60–10.63 are suitable for modeling viscosity up to the saturation limit in wide temperature ranges.

Viscosity data for electrolyte solutions are usually available only at room and moderately elevated temperatures (below 373 K and in some cases up to 423 K). A comprehensive collection of viscosity data is available in the compilation of Lobo and Quaresma (1989). The system NaCl–H_2O appears to be the only solution for which data are available for higher temperatures (up to 473 K (Kestin and Shankland, 1984) and a limited number of experimental points up to 629 K (Semenyuk *et al.*, 1977)). To illustrate the behavior of the viscosity in this prototype system, Fig. 10.11 shows both absolute and relative viscosities as a function of concentration and temperature at saturation pressure. Also, Fig. 10.11

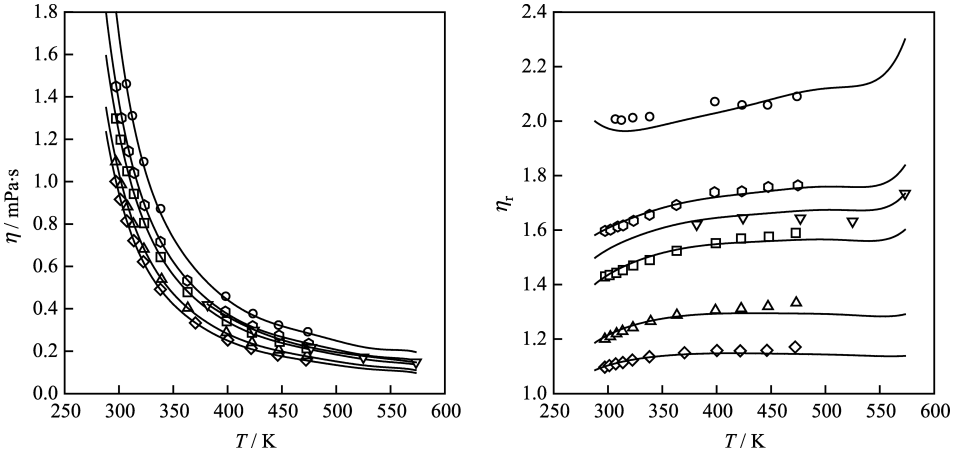

Fig. 10.11. Absolute and relative viscosity of the NaCl–H_2O solution as a function of temperature and concentration at saturation. The lines are obtained from Eqs. 10.60–10.63. The symbols denote experimental data: ◇ — 1.0661 m; △ — 2.0178 m; ● — 3.5161 m; ▽ — 4.045 m; ⌓ — 4.4538 m and ● — 6.038 m. The data for 1.0661, 2.0178, 3.5161, 4.4538 and 6.038 m solutions are from Kestin and Shankland (1984), those for 4.045 m are from Semenyuk *et al.* (1977).

illustrates the correlation of viscosity data using Eq. 10.60. This correlation was performed using multiple data sets from the literature (Lobo and Quaresma, 1989; Kestin and Shankland, 1984; Semenyuk *et al.*, 1977), which explains some small systematic deviations from the data at high concentrations (Lobo and Quaresma, 1989). The average deviation of the fit is 0.41% for a total of 302 experimental points.

In addition to the temperature and concentration dependence (*cf.* Fig. 10.11), the viscosity of electrolyte solutions exhibits a weak density dependence (*cf.* Kestin and Shankland (1984) and references cited therein). The density dependence results in a viscosity increment that is usually small at room temperature (0.2–1.8% for a pressure increment from saturation to ca. 30 MPa), but becomes more substantial at higher temperatures (2–4.5% at 473 K in the same pressure range).

10.7. Thermal Conductivity of Electrolyte Solutions

Most of the data on the thermal conductivity of electrolyte solutions at high temperature and pressure were reported during the last decade by Abdulagatov and Magomedov (2000) up to 473 K and 100 MPa. The systems studied include LiCl, NaCl, KCl, LiBr, KBr, KI, NaI, $MgCl_2$, $CaCl_2$, $CdCl_2$, $CoCl_2$, $SrCl_2$, $ZnCl_2$, $CdBr_2$, ZnI_2, $Sr(NO_3)_2$, K_2CO_3 and BaI_2. A few electrolytes ($Zn(NO_3)_2$, $CaCl_2$ and NaCl) were studied up to 573 K (Azizov and Magomedov, 1999; Abdullaev *et al.*, 1998).

In very dilute solutions, the ion–ion interaction contribution to the thermal conductivity (Bearman, 1964) is of the order of κ_D^3 (κ_D is the inverse Debye length) or $c^{3/2}$, showing a behavior quite different from that found for the electrical conductivity and viscosity in the concentration range where the Debye–Hückel theory is valid. However, in practice the thermal conductivity of dilute or moderately concentrated electrolyte solutions is described by a simple linear equation in the molar concentration proposed by Riedel (1951) at room temperature:

$$\lambda = \lambda_0 + \sum_i \alpha_i c_i \tag{10.64}$$

where λ_0 is the thermal conductivity of pure water and α_i is the contribution of ion i. McLaughlin (1964) extended this equation to 373 K by assuming that the thermal conductivity of the electrolyte solutions has the same temperature dependence as pure water. In terms of the salt molality, m, the equation proposed by McLaughlin for the thermal conductivity (in $W{\cdot}m^{-1}{\cdot}K^{-1}$) is:

$$\lambda(T,m) = \frac{1.1622\lambda_0(T)}{\lambda_0(T_0)}\left[0.515 - \alpha_s \frac{1000\rho(T,m)m}{1000 + M_s m}\right] \tag{10.65}$$

where ρ is the mass density of the solution, M_s the molar mass of the salt, α_s the sum of the α coefficients of the anion and cation, λ_0 is the thermal conductivity of pure water and $T_0 = 293$ K.

The thermal conductivities of the salt solutions decrease with increasing concentration, except for NaF, Na_2CO_3, Na_2SO_4, Na_3PO_4 and some alkaline hydroxides (Li, Na and K). The coefficients α_i are tabulated for several ions and they are negative for most of the ions, except for OH^-, F^-, SO_4^{2-}, PO_4^{3-} and CrO_4^{2-}.

Nagasawa *et al.* (1983) analyzed Eq. 10.65 for the case of NaCl solutions in the range 273–353 K and concentrations up to 5 $mol{\cdot}kg^{-1}$ and concluded that the disagreement between experimental and calculated values is 2% at most.

For all the electrolyte solutions studied up to 100 MPa, the thermal conductivity at constant temperature and concentration increases almost linearly with pressure (Nagasawa *et al.*, 1983; Abdulagatov and Magomedov, 2001) with a slope quite similar to that observed for pure water. In order to assess the pressure dependence of the thermal conductivity of electrolyte solutions, DiGuilio and Teja (1992) proposed a correlation which allows calculating the thermal conductivity of the solution at pressure p by knowing its thermal conductivity at 0.1 MPa:

$$\lambda(p,m) = \lambda(p_0,m)\frac{\lambda_0(p)}{\lambda_0(p_0)} \tag{10.66}$$

where λ_0 is the thermal conductivity of pure water and $p_0 = 0.1$ MPa. It was found that this simple correlation could reproduce experimental values for several electrolytes within 2% (Abdulagatov and Magomedov, 1998).

The temperature dependence of the thermal conductivity at constant pressure and concentration is more complex but it shows a common pattern for all the electrolytes studied up to 573 K. Along each isobar–isopleth, the thermal conductivity has a maximum at a temperature between 400 and 420 K, which is almost independent of pressure. This behavior mimics that observed for pure water as a function of temperature (see Chapter 1).

Abdulagatov and Magomedov (1997) proposed an empirical equation to describe the temperature, pressure and concentration dependence of the thermal conductivity of electrolyte solutions using only one electrolyte-dependent adjustable parameter. The equation is written in the form of a correction to λ_0, the thermal conductivity of pure water, and it is able to fit experimental results with reasonable accuracy. However, we discourage its use because the thermal conductivity of water is represented by a polynomial equation that yields values of λ_0 different from those obtained with the IAPWS Release for this property (IAPWS, 1998).

10.8. Multicomponent Ionic Solutions

Almost all systems encountered in industry or in natural environments are multicomponent. At the same time, the vast majority of experimental data, particularly at elevated temperatures, is for single-solute systems. Moreover, many theories that have been developed for predicting transport properties are applicable only to binary solutions. For example, this is the case for the MSA theories for the concentration dependence of electrical conductivity and self-diffusivity and for the semi-empirical model for calculating mutual diffusivity presented in previous sections. Therefore, it is important to have reliable methods for predicting the properties of multicomponent systems using the properties — either experimental or computed — of single-solute systems. In this section, we discuss such methods for electrical conductivity, diffusivity and viscosity.

10.8.1. Electrical Conductivity

To calculate the electrical conductivity of multicomponent mixtures, it is necessary to use a mixing rule that utilizes the conductivities, either experimentally obtained or calculated, of binary subsystems containing one cation and one anion. The functional form of the mixing rule should be guided by its empirical effectiveness and should be suitable for use in conjunction with theories for binary electrolyte solutions. For example, Miller (1996) reviewed several possible mixing rules for two-solute systems (*e.g.*, $NaCl + MgCl_2 + H_2O$). Such mixing rules can be written in terms of various solute fractions (molar,

equivalent or ionic strength) and the specific conductivity of constituent binary subsystems, *i.e.*,

$$\kappa(K) = a_1\kappa_1(K) + a_2\kappa_2(K) \tag{10.67}$$

where a_1 and a_2 are the fractions of binary subsystems 1 and 2, respectively, and the specific conductivities of the binary subsystems (*i.e.*, κ_1 and κ_2) are evaluated at constant concentration (K), which can be either constant total molarity, constant equivalent concentration or constant ionic strength.

Anderko and Lencka (1997) developed a general mixing rule for multicomponent systems by considering plausible ways of averaging the contributions of constituent binary cation–anion pairs. This mixing rule takes the form:

$$\kappa = c_{\text{eq}} \sum_{M=1}^{N_C} \sum_{X=1}^{N_A} f_M f_X [\lambda_{M(X)}(I) + \lambda_{X(M)}(I)] = c_{\text{eq}} \sum_{M=1}^{N_C} \sum_{X=1}^{N_A} f_M f_X \Lambda^0_{MX}(I) \tag{10.68}$$

where c_{eq} is the total equivalent concentration, f_M and f_X are the equivalent fractions of the cation and anion, respectively, $\lambda_{M(X)}$ is the conductivity of cation M in the presence of anion X, $\lambda_{X(M)}$ is the conductivity of anion X in the presence of cation M, and N_C and N_A are the total numbers of cations and anions, respectively. The equivalent fractions are defined as

$$f_i = \frac{|z_i| c_i}{c_{\text{eq}}} \tag{10.69}$$

and the equivalent concentration c_{eq} is given by

$$c_{\text{eq}} = \sum_{M}^{N_C} c_M |z_M| = \sum_{X}^{N_A} c_X |z_X|. \tag{10.70}$$

The conductivities $\lambda_{M(X)}$ and $\lambda_{X(M)}$ are defined at constant molar ionic strength I. For this purpose, these quantities are calculated at the concentrations of the ions in a binary pair MX given by:

$$c_M = \frac{2I}{|z_M|(|z_M| + |z_X|)}; \qquad c_X = \frac{2I}{|z_X|(|z_M| + |z_X|)}. \tag{10.71}$$

Eq. 10.71 has been derived to satisfy the condition of a constant ionic strength.

This mixing rule gives accurate predictions for the electrical conductivity of mixed systems. This is illustrated in Fig. 10.12 for the system $NaCl–MgCl_2–H_2O$. In this example, the conductivities in the binary subsystems $Na^+–Cl^-$ and $Mg^{2+}–Cl^-$ were calculated using the MSA model with effective ionic radii (Anderko and Lencka, 1997) and the conductivities of the mixed system were obtained using Eqs. 10.68–10.71. There are no data to test the mixing rule at high temperatures over substantial concentration ranges. However, there is every

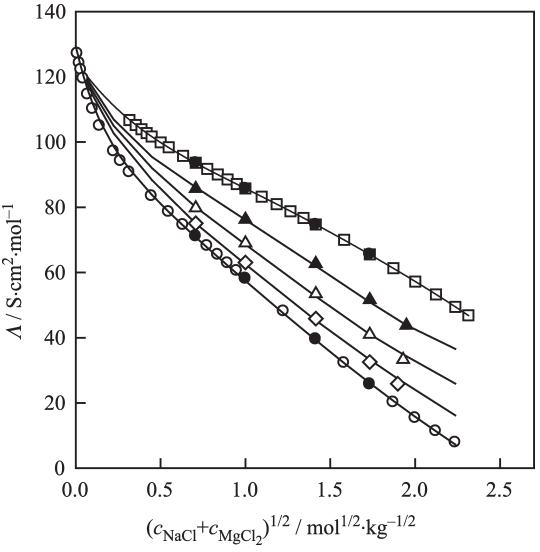

Fig. 10.12. Application of Eqs. 10.68–10.71 to calculate electrical conductivity in the mixed system NaCl–$MgCl_2$–H_2O at 298.15 K. The lines are calculated from the model and labeled according to the NaCl:$MgCl_2$ ratio. The symbols denote experimental data for fixed NaCl:$MgCl_2$ ratios: ● — 1:0 (Bianchi *et al.*, 1989); ● — 1:0 (Chambers *et al.*, 1956); ● — 3:1 (Bianchi *et al.*, 1989); △ — 1:1 (Bianchi *et al.*, 1989); ◇ — 1:3 (Bianchi *et al.*, 1989); ● — 0:1 (Bianchi *et al.*, 1989) and ● — Miller (1966).

indication that the mixing rule should be equally applicable at high and low temperatures (Sharygin *et al.*, 2001).

Recently, Sharygin *et al.* (2001) have shown that Eq. 10.68 is a special case of a general mixing rule that was originally developed by Reilly and Wood (1969) for thermodynamic properties such as volumes, enthalpies and Gibbs energies of mixing. In its version for electrical conductivity, the Reilly–Wood mixing rule contains two additional terms, which represent cation(1)–cation(2)–anion and cation–anion(1)–anion(2) mixing effects:

$$\kappa = c_{\mathrm{eq}} \sum_{M=1}^{N_{\mathrm{C}}} \sum_{X=1}^{N_{\mathrm{A}}} f_M f_X \Lambda^0_{MX}(I) + RTc^2_{\mathrm{eq}} \sum_{M<N}^{N_{\mathrm{C}}} \sum_{Y=1}^{N_{\mathrm{A}}} f_M f_N f_Y k^Y_{MN} + RTc^2_{\mathrm{eq}} \sum_{M=1}^{N_{\mathrm{C}}} \sum_{X<Y}^{N_{\mathrm{A}}} f_M f_X f_Y k^M_{XY} \qquad (10.72)$$

where k^Y_{MN} and k^M_{XY} are ternary mixing parameters, which can be evaluated if very accurate data are available for the mixed systems MY–NY–H_2O and MX–MY–H_2O, respectively. The first term of this mixing rule is equivalent to Eq. 10.68. For practical applications to electrical conductivity of multicomponent solutions, it appears that the first term is entirely sufficient (*cf.* Fig. 10.12).

10.8.2. Diffusion

As with electrical conductivity, theories for diffusion coefficients in multicomponent systems are available only for dilute solutions (Onsager and Kim, 1957; Onsager and Fuoss, 1932). For more concentrated solutions, it is necessary to use semi-empirical mixing rules. In this chapter, we discuss such mixing rules for self- and mutual diffusion coefficients.

10.8.2.1. Self-Diffusion

In the case of self-diffusion, the Stefan–Maxwell formalism of diffusion (Eq. 10.20) has been used to derive a mixing rule that makes it possible to predict self-diffusivities of both ionic and neutral solution species in multicomponent solutions as long as they can be obtained for the constituent binary systems (*i.e.*, systems containing one salt or one molecular solute in water). To derive this mixing rule, Anderko and Lencka (1998) assumed that a multicomponent mixture contains N_C cations, N_A anions and N_N neutral solutes. Then, the cations and anions can be formally separated into $N_C N_A$ neutral solutions containing only one cation and one anion. Further, it can be assumed that each of such hypothetical solutions contains $n_{+(d)}$ moles of cations, $n_{-(d)}$ moles of anions and $n_{s(d)}$ moles of the solvent, where $d = 1, \ldots, N_C N_A$ is an index that identifies the hypothetical solution. Similarly, the neutral solutes can be placed into N_N hypothetical solutions, which contain n_l moles of the solute and $n_{s(l)}$ moles of the solvent ($l = 1, \ldots, N_N$). Then, the self-diffusivity in a multicomponent solution can be calculated as

$$D_i = \frac{n_T}{\sum_{d=1}^{N_C N_A} \frac{n_{s(d)} + n_{+(d)} + n_{-(d)}}{D_{i(d)}} + \sum_{l=1}^{N_N} \frac{n_{s(l)} + n_l}{D_{i(l)}}} \tag{10.73}$$

where the coefficients $D_{i(d)}$ and $D_{i(l)}$ are obtained for the constituent binary solutions at the same total number density as that of the multicomponent mixture. Although this mixing rule has been rigorously derived, it does not specify how the multicomponent solution of interest should be subdivided into hypothetical single-solute solutions. For this purpose, arbitrary assumptions have to be made. To define the quantities $n_{+(d)}$ and $n_{-(d)}$, it can postulated that the amounts of the cation and anion in the hypothetical single-solute solution should be proportional to the concentrations of the cation and the anion in the multicomponent solution. Furthermore, the hypothetical single-solute solution should be electrically neutral. Expressions that satisfy these conditions are given by Anderko and Lencka (1998).

10.8.2.2. Mutual Diffusion

Mutual diffusion in multicomponent systems has been extensively investigated using both the Fick (Eq. 10.17) and Stefan–Boltzmann (Eq. 10.20) diffusion formalisms. It should be noted that mutual diffusion in multicomponent solutions is not a simple extension of binary diffusion. When more than one salt is present in a solution, the restriction that anions and cations must diffuse with the same speed is lifted. This has important implications. On the phenomenological level, there may be a substantial modification in the main diffusion coefficients D_{ii} and large cross coefficients D_{ij} (*cf.* Eq. 10.17). On the molecular level, electrostatic interactions manifest themselves in both the electrophoretic and relaxation effects whereas mutual diffusion in a binary solution is affected only by the electrophoretic effect.

Diffusion in multicomponent systems can be comprehensively described using the Onsager phenomenological coefficients a_{ij}, which relate the flux of ion i (*i.e.*, $\mathbf{J}_i$) to the gradient of the electrochemical potential (Eq. 10.6). According to the ORR, Eq. 10.7, the matrix of the a_{ij} coefficients is symmetric (*i.e.*, $a_{ij} = a_{ji}$). Thus, each binary subsystem is characterized by three coefficients: $a_{\text{cation}-\text{cation}}$, $a_{\text{anion}-\text{anion}}$ and $a_{\text{cation}-\text{anion}}$. The a_{ij} coefficients can be theoretically predicted only for very dilute multicomponent solutions (below 0.01 molal). Onsager and coworkers (Onsager and Fuoss, 1932; Onsager and Kim, 1957; Chen and Onsager, 1977) derived limiting expressions, which can be applied to compute a_{ij} using the limiting conductivities of species and the dielectric constant, viscosity and density of the solution.

For more concentrated solutions, the a_{ij} coefficients can be calculated only from experimental data. Miller (1966, 1967a,b) performed a comprehensive analysis of the relationship between the Onsager coefficients and observable transport properties. In particular, Miller (1966) has derived a rigorous expression for calculating these coefficients when electrical conductivity (Λ), transference number (t_i) and mutual diffusivity (D_v) data are available. Then, the a_{ij} coefficients can be calculated for a binary solution as:

$$a_{ij} = \frac{t_i t_j \kappa}{F^2 z_i z_j} + \frac{\nu_i \nu_j c D_v}{RT\nu\left(1 + (m\mathrm{d}\ln\gamma)/(\mathrm{d}m)\right)} \tag{10.74}$$

where ν_i are the stoichiometric coefficients of ionization of the salt, $\nu = \nu_i + \nu_j$, and γ is the molality-based activity coefficient.

If all a_{ij} coefficients are known for a multicomponent solution, the Fick's-law diffusion coefficients D_{ij} (*cf.* Eq. 10.17) can be computed. These diffusion coefficients can be computed on an ionic basis (*i.e.*, when i and j denote ions) and on a neutral solute basis (*i.e.*, when i and j denote salts). Expressions for the ionic mutual diffusion coefficients have been obtained by Felmy and Weare (1991)

following earlier work by Lasaga (1979) and Miller (1967a,b):

$$D_{ij} = RTV\left[\sum_{k=1}^{N} a_{ik}\left(h_{kj} - h_{k0}\frac{\bar{V}_j}{\bar{V}_0}\right) - \frac{\sum_{m=1}^{N}\sum_{n=1}^{N}\sum_{k=1}^{N} a_{ik}z_k z_m a_{mn}\left(h_{nj} - h_{n0}(\bar{V}_j/\bar{V}_0)\right)}{\sum_{m=1}^{N}\sum_{n=1}^{N} z_m z_n a_{mn}}\right] \tag{10.75}$$

where

$$h_{kj} = \frac{\partial \ln a_k}{\partial n_j} \tag{10.76}$$

and $\bar{V}_i$ is the partial molal volume of species i, V is the solution volume, a_k is the activity of species k and the subscript 0 represents the solvent.

Expressions for calculating the diffusion coefficients D_{ij} of salts (rather than ions) in terms of the Onsager a_{ij} coefficients have been developed by Miller (1967a,b) and Leaist and Lyons (1980). Such coefficients can be directly compared with experimental data, especially for ternary solutions.

The a_{ij} coefficients are usually strong functions of concentration. Thus, their concentration dependence has to be accurately known before they can be applied to multicomponent systems. According to Miller (1967a,b), the a_{ij} coefficients should be evaluated at the same normality in the binary as in the multicomponent system. To evaluate the a_{ij} coefficients, a considerable amount of accurate experimental data (*i.e.*, electrical conductivity, transference numbers and binary mutual diffusivity) is necessary. While the coefficients for cation–anion pairs can be obtained from data for binary solutions, those for cation–cation or anion–anion pairs should be obtained from common-ion ternary data. Miller (1967a,b) developed mixing rules in order to evaluate such parameters without having to resort to ternary data. These mixing rules were further verified by Felmy and Weare (1991), Kim (1982) and Kim *et al.* (1973).

Even with this mixing rule, prediction of mutual diffusivities requires the simultaneous availability of diffusion coefficients, electrical conductivity and transference numbers for constituent binary subsystems at the temperature of interest. Such data are available for a limited number of systems, usually only at room or slightly elevated temperatures (Rard and Miller, 1987, 1988; Rard *et al.*, 1996). This severely limits the usefulness of this methodology, especially at high temperatures. An alternative, simpler approach based on the Stefan–Maxwell formalism has been proposed by Pinto and Graham (1987). However, a practical method for predicting mutual diffusion coefficients at high temperatures remains to be developed.

10.8.3. Viscosity

Unlike electrical conductivity and diffusivity, viscosity can be calculated from a model that is directly applicable to multicomponent solutions. For dilute solutions, the Jones–Dole equation (Eq. 10.56) can be rigorously written for multicomponent systems because of the additivity of the B coefficients for individual ions. Also, the semi-empirical species–species interaction contribution that extends the Jones–Dole equation to concentrated solutions (Eq. 10.60) is given in a multicomponent form. Lencka *et al.* (1998) verified the performance of this equation for selected systems containing multiple salts and obtained good agreement with experimental data.

References

Abdulagatov, I.M. and Magomedov, U.B., *Int. J. Thermophys.*, **15**, 401–407 (1994).

Abdulagatov, I.M. and Magomedov, U.B., *Ber. Bunsen-Ges. Phys. Chem.*, **101**, 708–711 (1997).

Abdulagatov, I.M. and Magomedov, U.B., *Ind. Eng. Chem. Res.*, **37**, 4883–4888 (1998).

Abdulagatov, I.M. and Magomedov, U.B., *Fluid Phase Equilib.*, **171**, 243–252 (2000), and references therein.

Abdulagatov, I.M. and Magomedov, U.B., *J. Solution Chem.*, **30**, 223–235 (2001).

Abdullaev, K., El'darov, V.S. and Mustafaev, A.M., *High-Temp. High-Press.*, **36**, 375–378 (1998).

Anderko, A. and Lencka, M.M., *Ind. Eng. Chem. Res.*, **36**, 1932–1943 (1997).

Anderko, A. and Lencka, M.M., *Ind. Eng. Chem. Res.*, **37**, 2878–2888 (1998).

Azizov, N.D. and Magomedov, U.B., *High-Temp. High-Press.*, **37**, 649–651 (1999).

Bagchi, B. and Biswas, R., *Acc. Chem. Res.*, **31**, 181–187 (1998).

Balbuena, P.B., Johnston, K.P., Rossky, P.J. and Hyun, J.-K., *J. Phys. Chem.*, **102**, 3806–3814 (1998).

Baruël, P., Danish Atomic Energy Commission Research Establishment. Risø Report No. 264, 1972 and No. 280, 1973.

Bearman, R.J., *J. Chem. Phys.*, **41**, 3924–3925 (1964).

Becker, P. and Bilal, B.A., *J. Solution Chem.*, **14**, 367–373 (1985).

Berendsen, H.J.C., Grigera, J.R. and Straatsma, T.P., *J. Phys. Chem.*, **91**, 6269–6271 (1987).

Bernard, O., Kunz, W., Turq, P. and Blum, L., *J. Phys. Chem.*, **96**, 398–403 (1992).

Berry, R.S., Rice, S.A. and Ross, J., *Physical Chemistry*, 2nd edn. Oxford University Press, Oxford, 2000.

Bianchi, H., Corti, H.R. and Fernández-Prini, R., *J. Solution Chem.*, **18**, 485–491 (1989).

Bianchi, H., Corti, H.R. and Fernández-Prini, R., *Rev. Sci. Instrum.*, **64**, 1636–1640 (1993).

Bianchi, H., Corti, H.R. and Fernández-Prini, R., *J. Solution Chem.*, **23**, 1203–1212 (1994).

Bianchi, H., Dujovne, I. and Fernández-Prini, R., *J. Solution Chem.*, **29**, 237–253 (2000).

Biswas, R. and Bagchi, B., *Chem. Phys. Lett.*, **290**, 223–228 (1998).

Boero, M., Terakura, K., Ikeshoji, T., Liew, C.C. and Parrinello, M., *J. Chem. Phys.*, **115**, 2219–2227 (2001).

Braun, B.M. and Weingärtner, H., *J. Phys. Chem.*, **92**, 1342–1346 (1988).

Brett, C.M.A. and Brett, A.M.O., *Electrochemistry, Principles, Methods and Applications*. Oxford University Press, Oxford, 1993.

Butenhoff, T.J., Goemans, M.G.E. and Buelow, S.J., *J. Phys. Chem.*, **100**, 5982–5992 (1996).

Chambers, J.F., Stokes, J.M. and Stokes, R.H., *J. Phys. Chem.*, **60**, 985–986 (1956).

Chen, M. and Onsager, L., *J. Phys. Chem.*, **81**, 2017–2021 (1977).

Chhih, A., Turq, P., Bernard, O., Barthel, J. and Blum, L., *Ber. Bunsen-Ges. Phys. Chem.*, **98**, 1516–1525 (1994).

Chin, D.T. and Tsang, C.H., *J. Electrochem. Soc.*, **125**, 1461–1470 (1978).

Cussler, E.L., *Diffusion: Mass Transfer in Fluid Systems*, 2nd edn. Cambridge University Press, Cambridge, 1997.

Debye, P. and Hückel, E., *Phys. Z.*, **24**, 185–206 (1924).

Dietz, F.J., de Grot, J.J. and Franck, E.U., *Ber. Bunsen-Ges. Phys. Chem.*, **85**, 1005–1012 (1981).

DiGuilio, R.M. and Teja, A.S., *Ind. Eng. Chem. Res.*, **31**, 1081–1085 (1992).

Dudziak, K.H. and Franck, E.U., *Ber. Bunsen-Ges. Phys. Chem.*, **70**, 1120–1128 (1966).

Q5 Easteal, A.J., Price, W.E. and Woolf, L.A., *J. Chem. Soc., Faraday Trans. I*, **85**, 1091–1097 (1989).

Felmy, A. and Weare, J.H., *Geochim. Cosmochim. Acta*, **55**, 113–131 (1991).

Fernández-Prini, R., *Trans. Faraday Soc.*, **65**, 3311–3313 (1969).

Fernández-Prini, R. In: Covington, A.K. and Dickinson, T. (Eds.), *Physical Chemistry of Organic Solvent Systems, Chapter 5, Part 1: Conductance*. Plenum Press, New York, 1973.

Fernández-Prini, R. and Justice, J.-C., *Pure Appl. Chem.*, **56**, 541–547 (1984).

Flarsheim, W.M., Tsou, Y., Trachtenberg, I., Johnston, K.P. and Bard, A.J., *J. Phys. Chem.*, **90**, 3857–3862 (1986).

Franck, E.U., *Z. Phys. Chem.*, **8**, 92–106 (1956).

Franck, E.U., Savolainen, J.E. and Marshall, W.L., *Rev. Sci. Instrum.*, **33**, 115–117 (1962).

Frantz, J.D. and Marshall, W.L., *Am. J. Sci.*, **282**, 1666–1693 (1982).

Frantz, J.D. and Marshall, W.L., *Am. J. Sci.*, **284**, 651–667 (1984).

Fuoss, R. and Hsia, K.-L., *Proc. Natl Acad. Sci. USA*, **57**, 1550–1557 (1967).

Fuoss, R. and Onsager, L., *J. Phys. Chem.*, **61**, 668–682 (1957).

Goemans, M.G.E., Gloyna, E.F. and Buelow, S.J., *Proceedings of the Second International Symposium on Environmental Applications of Advanced Oxidation Technologies*. EPRI, Palo Alto, CA, 1996.

Graham, E.E. and Dranoff, J.S., *Ind. Eng. Chem. Fundam.*, **21**, 360–365 (1982).

Gruszkiewicz, M.S. and Wood, R.H., *J. Phys. Chem. B*, **101**, 6547–6559 (1997).

Haase, R., *Thermodynamics of Irreversible Processes*. Dover Publ. Inc., New York, 1990.

Hansen, J.P. and McDonald, I.R., *Theory of Simple Liquids*. Academic Press, New York, 1976, pp. 236–242.

Harned, H.S. and Owen, B.B., *The Physical Chemistry of Electrolytic Solutions*, 3rd edn. Reinhold, New York, 1950.

Hartley, G.S. and Crank, J., *Trans. Faraday Soc.*, **45**, 801–818 (1949).

Ho, P.C. and Palmer, D.A., *J. Solution Chem.*, **25**, 711–729 (1996).

Ho, P.C. and Palmer, D.A., *Geochim. Cosmochim. Acta*, **61**, 3027–3040 (1997).

Ho, P.C. and Palmer, D.A., *J. Chem. Eng. Data*, **43**, 162–170 (1998).

Ho, P.C., Palmer, D.A. and Mesmer, R.E., *J. Solution Chem.*, **23**, 997–1018 (1994).

Ho, P.C., Bianchi, H., Palmer, D.A. and Wood, R.H., *J. Solution Chem.*, **29**, 217–235 (2000a).

Ho, P.C., Palmer, D.A. and Wood, R.H., *J. Phys. Chem. B*, **104**, 12084–12089 (2000b).

Ho, P.C., Palmer, D.A. and Gruszkiewicz, M.S., *J. Phys. Chem. B*, **105**, 1260–1266 (2001).

Q5 Holz, M., Heil, S.R. and Sacco, A., *Phys. Chem. Chem. Phys.*, **2**, 4740–4742 (2000).

Horvath, A.L., *Handbook of Aqueous Electrolyte Solutions*. Ellis Horwood, Chichester, 1985.

Hubbard, J. and Onsager, L., *J. Chem. Phys.*, **67**, 4850–4857 (1977).

Hyun, J.-K., Johnston, K.P. and Rossky, P.J., *J. Phys. Chem. B*, **105**, 9302–9307 (2001).

IAPWS, *Release on the Ion Product of Water Substance*. See Chapter 1 for information on obtaining IAPWS Releases, 1980.

IAPWS, *Revised Release on the IAPS Formulation 1985 for the Thermal Conductivity of Ordinary Water Substance*. See Chapter 1 for information on obtaining IAPWS Releases, 1998.

Ibuki, K., Ueno, M. and Nakahara, M., *J. Phys. Chem. B*, **104**, 5139–5150 (2000).

Ikeuchi, H., Hayafuji, M., Aketagawa, Y., Taki, J. and Sato, G., *J. Electroanal. Chem.*, **396**, 553–556 (1995).

Jones, G. and Dole, M., *J. Am. Chem. Soc.*, **51**, 2950–2964 (1929).

Justice, J.-C. In: Conway, B.E., Bockris, J.O.M. and Yeager, E. (Eds.), *Comprehensive Treatise of Electrochemistry*. Plenum Press, New York, Vol. 4, 1983, chapter 3.

Kaminsky, M., *Z. Phys. Chem.*, **12**, 206–231 (1957).

Kestin, J. and Shankland, I.R., *Int. J. Thermophys.*, **5**, 241–263 (1984).

Kestin, J., Khalifa, H.E. and Correia, R.J., *J. Phys. Chem. Ref. Data*, **10**, 57–70 (1981a).

Kestin, J., Khalifa, H.E. and Correia, R.J., *J. Phys. Chem. Ref. Data*, **10**, 71–87 (1981b).

Kim, H., *J. Chem. Eng. Data*, **27**, 255–256 (1982).

Kim, H., Reinfelds, G. and Gosting, L.J., *J. Phys. Chem.*, **77**, 934–940 (1973).

Kimura, Y., Kanda, D., Terazima, M. and Hirota, N., *Ber. Bunsen-Ges. Phys. Chem.*, **99**, 196–203 (1995).

Koneshan, S. and Rasaiah, J.C., *J. Chem. Phys.*, **113**, 8125–8137 (2000).

Korosi, A. and Fabuss, B.M., *J. Chem. Eng. Data*, **13**, 548–552 (1968).

Krynicki, K., Green, C.D. and Sawyer, D.W., *Faraday Discuss. Chem. Soc.*, **66**, 199–208 (1979).

Lamb, W.J., Hoffman, G.A. and Jonas, J., *J. Chem. Phys.*, **74**, 6875–6880 (1981).

Lasaga, A., *Am. J. Sci.*, **279**, 324–346 (1979).

Leaist, D.G. and Lyons, P.A., *Aust. J. Chem.*, **33**, 1869–1887 (1980).

Lee, S.H. and Cummings, P.T., *J. Chem. Phys.*, **112**, 864–869 (2000).

Lee, W. and Wheaton, R., *J. Chem. Soc., Faraday Trans. II*, **74**, 743–766 (1978).

Lee, S.H., Cummings, P.T., Simonson, J.M. and Mesmer, R.E., *Chem. Phys. Lett.*, **293**, 289–294 (1998).

Lencka, M.M., Anderko, A., Sanders, S.J. and Young, R.D., *Int. J. Thermophys.*, **19**, 367–378 (1998).

Le Neindre, B., Tufeu, R., Bury, P. and Sengers, J.V., *Ber. Bunsen-Ges. Phys. Chem.*, **77**, 262–275 (1973).

Lindsay, W.T., *Estimation of Diffusion Coefficients for Electrolytes in Hot Water*, Topical Report for Research Project S146-1. EPRI, Palo Alto, CA, 1980.

Liu, C.-T. and Lindsay, W.T., *J. Solution Chem.*, **1**, 45–69 (1971).

Liu, C., Snyder, S.R. and Bard, A.J., *J. Phys. Chem. B*, **101**, 1180–1185 (1997).

Lobo, V.M.M. and Quaresma, J.L., *Handbook of Electrolyte Solutions, Parts A and B*. Elsevier, Amsterdam, 1989.

Marcus, Y., *Ion Solvation*. Wiley, New York, 1985.

Marcus, Y., *Ion Properties*. Marcel Dekker, New York, 1997.

Marshall, W.L., *J. Chem. Phys.*, **87**, 3639–3643 (1987a).

Marshall, W.L., *J. Chem. Eng. Data*, **32**, 221–226 (1987b).

Marshall, W.L. and Franck, E.U., *J. Phys. Chem. Ref. Data*, **10**, 295–304 (1981).

Marshall, W., Frantz, J.D. In: Ulmer, G.C. and Barnes, H.L. (Eds.), *Hydrothermal Experimental Techniques*. Wiley-Interscience, New York, 1987, chapter 11.

McBreen, J., O'Grady, W.E. and Richter, R., *J. Electrochem. Soc.*, **131**, 1215–1216 (1984).

McDonald, A.C., Fan, F.F. and Bard, A.J., *J. Phys. Chem.*, **90**, 196–202 (1986).

McLaughlin, E., *Chem. Rev.*, 389–428 (1964).

Miller, D.G., *J. Phys. Chem.*, **70**, 2639–2659 (1966).

Miller, D.G., *J. Phys. Chem.*, **71**, 616–632 (1967a).

Miller, D.G., *J. Phys. Chem.*, **71**, 3588–3592 (1967b).

Miller, D.G., *J. Phys. Chem.*, **100**, 1220–1226 (1996).

Miller, D.G., Rard, J.A., Eppstein, L.B. and Albright, J.G., *J. Phys. Chem.*, **88**, 5739–5748 (1984).

Mills, R., *J. Phys. Chem.*, **61**, 1631–1634 (1957).

Q5 Mills, R., *J. Phys. Chem.*, **77**, 685–688 (1973).
Mills, R. and Lobo, V.M.M., *Self-Diffusion in Electrolyte Solutions*. Elsevier, Amsterdam, 1989.
Moorcroft, M.J., Lawrence, N.S., Coles, B.A., Compton, R.G. and Trevani, L.N., *J. Electroanal. Chem.*, **506**, 28–33 (2001).
Nagasawa, Y., Okada, H., Suzuki, J. and Nagashima, A., *Ber. Bunsen-Ges. Phys. Chem.*, **87**, 859–866 (1983).
Nakahara, M., Török, T., Takisawa, N. and Osugi, J., *J. Chem. Phys.*, **76**, 5145–5149 (1982).
Noyes, A.A., Carnegie Institution of Washington, DC, USA, Publication No. 63, 1907.
Oelkers, E.H. and Helgeson, H.C., *Geochim. Cosmochim. Acta*, **52**, 63–85 (1988).
Okada, K., Imashuku, Y. and Yao, M., *J. Chem. Phys.*, **107**, 9302–9311 (1997).
Okada, K., Yao, M., Hiejina, Y., Kohno, H. and Kajihara, Y., *J. Chem. Phys.*, **110**, 3026–3036 (1999).
Onsager, L., *Phys. Z.*, **28**, 277–286 (1927).
Onsager, L., *Phys. Rev.*, **33**, 2265–2279 (1931a).
Onsager, L., *Phys. Rev.*, **37**, 405–426 (1931b).
Onsager, L., *Phys. Rev.*, **38**, 2265–2279 (1931c).
Onsager, L., *Ann. N.Y. Acad. Sci.*, **46**, 241–265 (1945).
Onsager, L. and Fuoss, R.M., *J. Phys. Chem.*, **36**, 2689–2778 (1932).
Onsager, L. and Kim, S.K., *J. Phys. Chem.*, **61**, 215–229 (1957).
Out, D.J.P. and Los, J.M., *J. Solution Chem.*, **9**, 19–35 (1980).
Padua, A.A.H., Fareleira, J.M.N.A., Calado, J.C.G. and Wakeham, W.A., *Int. J. Thermophys.*, **17**, 781–802 (1996).
Pinto, N.G. and Graham, E.E., *AIChE J.*, **33**, 436–443 (1987).
Pitts, E., *Proc. R. Soc.*, **217A**, 41–48 (1953).
Pitzer, K.S., *J. Am. Chem. Soc.*, **102**, 2902–2906 (1980).
Pitzer, K.S. and Simonson, J.M., *J. Phys. Chem.*, **90**, 3005–3009 (1986).
Qiu, F., Compton, R.G., Coles, B.A. and Marken, F., *J. Electroanal. Chem.*, **492**, 150–155 (2000).
Quist, A.S. and Marshall, W.L., *J. Phys. Chem.*, **69**, 2984–2987 (1965).
Quist, A.S. and Marshall, W.L., *J. Phys. Chem.*, **72**, 684–703 (1968).
Rard, J.A. and Miller, D.G., *J. Solution Chem.*, **8**, 701–716 (1979).
Rard, J.A. and Miller, D.G., *J. Phys. Chem.*, **91**, 4614–4620 (1987).
Rard, J.A. and Miller, D.G., *J. Phys. Chem.*, **92**, 6133–6140 (1988).
Rard, J.A., Albright, J.G., Miller, D.G. and Zeidler, M.E., *J. Chem. Soc., Faraday Trans.*, **92**, 4187–4197 (1996).
Re, M. and Laría, D., *J. Phys. Chem. B*, **101**, 10494–10505 (1997).
Reilly, P.J. and Wood, R.H., *J. Phys. Chem.*, **73**, 4292–4297 (1969).
Riedel, L., *Chem.-Ing.-Tech.*, **23**, 59–64 (1951).
Robinson, R.A., Stokes, R.H., *Electrolyte Solutions*. Butterworths, London, 1959.
Sawamura, S., Takeuchi, N., Kitamura, K. and Taniguchi, Y., *Rev. Sci. Instrum.*, **61**, 871–873 (1990).
Semenyuk, E.N., Zarembo, V.I. and Fedorov, M.K., *Zh. Prikl. Khim.*, **50**, 315–319 (1977).
Sharygin, A.C., Mokbel, I., Xiao, C. and Wood, R.H., *J. Phys. Chem. B*, **105**, 229–237 (2001).
Skaf, M.S. and Laría, D., *J. Chem. Phys.*, **113**, 3499–3502 (2000).
Smith, J.E. and Dismukes, E.B., *J. Phys. Chem.*, **68**, 1603–1606 (1964).
Q3 Smolyakov, B.S., *Handbook of Aqueous Electrolyte Solutions*. Ellis Horwood, Chichester, 1969, p. 262.
Smolyakov, B.S. and Veselova, G.A., *Elektrokhimiya*, **11**, 700–704 (1975).
Sweeton, F.H., Mesmer, R.H. and Baes, C.F. Jr., *J. Solution Chem.*, **3**, 191–214 (1974).
Tanaka, K. and Nomura, M., *J. Chem. Soc., Faraday Trans. I*, **83**, 1779–1783 (1987).
Taylor, R. and Krishna, R., *Multicomponent Mass Transfer*. Wiley-Interscience, New York, 1993.

Terazima, M., Okamoto, K. and Hirota, N., *J. Chem. Phys.*, **102**, 2506–2515 (1995).
Tham, M.K. and Gubbins, K.E., *J. Chem. Phys.*, **55**, 268–279 (1971).
Trevani, L.N., Calvo, E. and Corti, H.R., *J. Chem. Soc., Faraday Trans.*, **93**, 4319–4326 (1997).
Trevani, L.N., Calvo, E. and Corti, H.R., *Electrochem. Commun.*, **2**, 312–316 (2000).
Turq, P., Lantelme, F., Roumegous, Y. and Chemla, M., *Self-Diffusion in Electrolyte Solutions*. Elsevier, Amsterdam, 1971, pp. 101–104.
Turq, P., Blum, L., Bernard, O. and Kunz, W., *J. Phys. Chem.*, **99**, 822–827 (1995).
Tyrrell, H.J.V. and Harris, K.R., *Diffusion in Liquids*. Butterworths, London, 1984.
Vitagliano, *Handbook of Electrolyte Solutions, Part B*. Elsevier, Amsterdam, 1960, p. 1611.
Wakeham, W.A. and Zalaf, M., *Fluid Phase Equilib.*, **36**, 183–194 (1987).
Wishaw, B.F. and Stokes, R.H., *J. Am. Chem. Soc.*, **76**, 2065–2071 (1954).
Wojtowicz, J. and Conway, B.E., *J. Electroanal. Chem. B*, **13**, 333–342 (1967).
Wolynes, P.G., *Annu. Rev. Phys. Chem.*, **31**, 345–376 (1980).
Wood, R.H., Carter, R.W., Quint, J.R., Majer, V., Thompson, P.T. and Boccio, J.R., *J. Chem. Thermodyn.*, **26**, 225–249 (1994).
Wu, Y.C. and Koch, W.F., *J. Solution Chem.*, **20**, 391–401 (1991).
Xiao, C. and Wood, R.H., *J. Phys. Chem. B*, **104**, 918–925 (2000).
Zimmerman, G.H., Gruszkiewicz, M.S. and Wood, R.H., *J. Phys. Chem.*, **99**, 11612–11625 (1995).
Zwanzig, R., *J. Chem. Phys.*, **52**, 3625–3628 (1970).

Author Queries

JOB NUMBER: 4649

Title Transport properties in high temperature and pressure ionic solutions

Q1 Please check the name of the city added to the second and third affiliations.

Q2 Please check "Summary" has been changed to "Introduction" and subsequent sections have been renumbered.

Q3 Please check the edit made to the references Smolyakov (1969), Turq et al. (1971) and Vitagliano (1960).

Q4 Please provide volume number for reference McLaughlin (1964).

Q5 Author, these references are not cited in the text. Please add or delete from reference list. Easteal et al., 1989, Holz et al., 2000, Krynicki et al., 1979, Miller et al., 1984 and Mills, 1973.